Michigan State University

National Superconducting Cyclotron Laboratory

CANONICAL ENSEMBLES FROM CHAOS II: CONSTRAINED DYNAMICAL SYSTEMS

DIMITRI KUSNEZOV and AUREL BULGAC

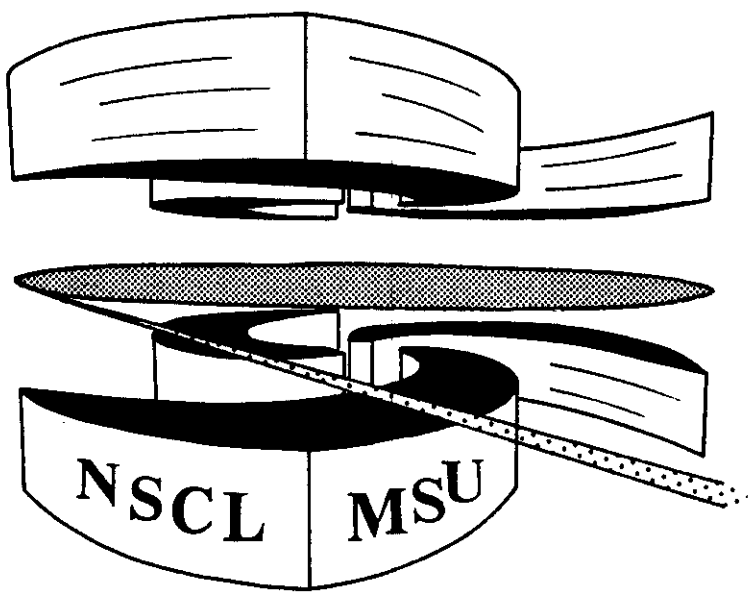

MSUCL-788 **JULY 1991**

MSUCL-788
July, 1991

CANONICAL ENSEMBLES FROM CHAOS II: CONSTRAINED DYNAMICAL SYSTEMS

DIMITRI KUSNEZOV[†] AND AUREL BULGAC

National *Superconducting Cyclotron Laboratory*
and Department *of* ***Physics*** and Astronomy,
Michigan State University, East Lansing, ***MI 48824-1321***

ABSTRACT

We present dynamical equations *of* motion *to* compute *thermodynamic properties of* constrained *dynamical systems. In* particular, *we examine systems that* can be described by generators of Lie algebras In this method, additional (non-compact) degrees of freedom are added *to the compact phase space to mock the effects of a heat* bath. *The* equations of motion *in this extended space are* ergodic, *and canonical ensemble averages* reduce *to* time averages over *the* classical *trajectory. We* compute *explicitly the* thermodynamic *properties of several simple systems, in: particular, Hamiltonians* with $SU(2)$ and $SU(3)$ symmetry.

[†] After Sept. 1, 1991, Center for Theoretical Physics, Yale University, New Haven, CT 06511.

1. INTRODUCTION

We have recently proposed methods to compute canonical ensemble averages for a classical system by extending the phase space to include two additional variables (pseudofriction coefficients) [1,2, 3] . These are here after refered to as I. Our methods are based on initial efforts by Nosé and Hoover [4] , which were modified to produce ergodic dynamics. In [5] we extended this approach to the case of a Brownian particle, where we develop a deterministic and time-reversal invariant description of its motion. The principle is to reduce the computation of thermal properties of arbitrary (possibly regular) many body systems to that of simple time averages. Historically, one of the main contributions of J.W. Gibbs was to demonstrate how time averages could be replaced by canonical ensemble averages. In order to evaluate the emerging multidimensional integrals various approaches have been developped: Monte Carlo technique, in particular the Metropolis algorithm [6] , stochastic quantization approach [7] , hybrid Monte Carlo method [8] , molecular dynamics techniques, often each one of these with a large number of variants. In all these approaches the multidimensional integrals are replaced with time averages over some trajectories (ergodicity always implied), i.e. doing exactly the opposite of what the founding fathers of statistical mechanics taught us to do. The Monte-Carlo (Metropolis) evaluation of the canonical ensemble integral generates a sequence of points which can be viewed as a trajectory in phase space, albeit a completely unphysical trajectory. In the stochastic quantization scheme one generates trajectories by solving a generalized Langevin equation in the phase space. The main deficiency of the method is that the effective rate of exploring the phase space is rather slow, since one models a diffusion process, the radius of the phase space volume scanned scales with time like $\propto \sqrt{t}$. In the hybrid Monte Carlo method, by combining deterministic Hamilton evolution with a "Metropolis hit" and a "momentum refresh" at the end of a trajectory one achieves a significantly faster rate of sampling the phase space. The methods in I and those discussed here, on the other hand, also rely on a trajectory in phase space. However, this trajectory is driven by the physical forces of the system together with thermal fluctuations. This allows additional dynamical information, not available in Monte-Carlo simulations, to be extracted if needed. These methods are completetly deterministic, without any dissipation and even time-reversal invariant. In I we proposed the following procedure. The canonical ensemble of an arbitrary unconstrained 2N dimensional classical system H coupled to a heat bath at temperature T can be simulated by replacing the infinite degress of freedom of the heat bath by two additional variables. This results in an extended 2N+2 dimensional space in which the equations of motion are non-Hamiltonian. By achieving ergodicity, the resulting algorithm is indepen-

dent of initial conditions and time averages of arbitrary operators are precisely equivalent to canonical ensemble averages. The coupling of the envisaged system H to the thermostat is not unique, and different forms of the couplings result in different time correlations of the phase space variables. Additionally, the relative time scales of the interaction with the thermal bath and the natural time scales of the system are naturally included in the formalism. Details and examples can be found in I. In [9] we applied this method to the XY-model and compared it against the hybrid Monte-Carlo method as well. The critical exponents, which characterize the so called critical slowing-down, are smaller in our method than in the hybrid Monte-Carlo approach. This indicates that the isothermal dymamics has the potential to be a even faster method of evaluating canonical ensemble averages than the method of choice nowdays in lattice gauge calculations.

In previous formulations, conserved quantities of the original Hamiltonian are only conserved on average in the extended phase space. However, there are a wide class of problems that fall into the category of constained dynamics, where the constraints must be preserved exactly at all times. A simple example is that of a spin 1/2 particle coupled to a heat bath. While the orientation of the spin will vary in time, the length of the particle spin must be conserved exactly at all times in both the original and extended system. It is straight forward to see that the methods of Nosé-Hoover and those of I do not apply to $SU(2)$. Consider the case of a classical rotator described by the Hamiltonian $H = J_z^2/2$. Since total angular momentum J^2 is conserved, the phase space is the 2-sphere S^2, can be parameterized by the canonical coordinates

$$q = J_z = J\cos\theta, \qquad p = -\phi, \qquad \{q,p\} = 1. \tag{1.1}$$

This set of coordinates is not defined globally, and in general different atlases are required for a global description of the dynamics. If one naively applies the Nosé-Hoover approach, one obtains the following equations of motion:

$$\begin{aligned} \dot{q} &= 0, \\ \dot{p} &= q - \zeta p, \\ \dot{\zeta} &= -\alpha T. \end{aligned} \tag{1.2}$$

Here ζ is the heat bath degree of freedom which is coupled to the momentum and T is the temperature. These equations show that the energy of the original system $H = q^2/2$ is conserved identically in the extended system, which clearly cannot lead to a canonical ensemble. There is another complication due to the compact character of the phase space, where in principle one must use several different atlases in order to avoid singularities of a particular coordinate

set (in the above example the poles). Even though the Hamilton equations of motion are easily translated from one atlas to another, the terms describing the coupling to the thermal bath do not seem to have obvious transformation properties and consequently the extended equations of motion are undefined under such a transformation. Hence, our concern in this article is the extension of our previous algorithm to such constrained dynamical systems [1, 3] . The class of constrained dynamical systems is very big: classical spin models, path integral formulation of spin problems [12] , gauge field theories [13] , algebraic models of nuclear collective or molecular motion, etc. Our examples will focus on a particular realization of the problem, useful in itself, and containing the essential ingredients of a general constrained situation. We focus on Hamiltonians that can be written in terms of generators of a Lie algebra. The constraints in this case correspond to the Casimir invariants of the algebra. At the moment we also restrict the discussion to classical limits of Lie algebras as detailed in Ref. 10. Classical limits play important roles for many reasons. For example, wave functions are concentrated along classical trajectories. Often a very accurate description of quantum phenomena can be inferred from classical trajectories together with relatively small quantum fluctuations. Once there is an understanding of the classical limit, the quantum situation can be recovered through path integral methods as well. Of course, one can envision situations where one does not wish to conserve the Casimir invariants, or, in other words, maintain a fixed representation of the algebra. This class of problem falls more naturally into the framework of unconstrained dynamics as discussed in *I*.

As mentioned above, a manifestation of exactly conserved quantities in the classical limit of Lie algabras is a compact phase space [10] . The Casimir invariants impose constraints on the generators of the Lie algebra (which are noncanonical coordinates in the classical limit), inducing a topology on the phase space. On these curved phase spaces, previous methods of producing ergodic trajectories in an extended phase space are no longer valid, as illustrated in Eq. (1.2). A modified Liouville equation must be defined in which the curved geometry of the phase space is explicitly taken into account. That is, some care must be taken to ensure that chaotic trajectories are limited to the classical phase space manifold, and these do not wander into regions where the Casimirs are not conserved. The development of these methods parallels our treatment of classical systems in *I*. A very nice feature of these constrained methods is that the symmetries of the problem are built into the equations of motion and hence they are preserved throughout the time evolution of the system. This approach is similar to the standard treatment of classical constrained systems, in which one constructs the Dirac brackets [11] , that preserves the constraints, once these are known.

This paper is outlined as follows. In Section 2, we review the geometry of the classical phase space of Lie algebras in the context of Ref. [10] . In discussing the classical Poisson structure, the constraints due to the Casimir invariants will be seen to arise naturally in the formulation. In Section 3, we review basic definitions in chaos used throughout this article. In Section 4, the method of adding the heat bath degrees of freedom to the phase space is discussed. A Liouville equation is presented and the equations of motion are derived. Section 5 explicitly details the method for systems with $SU(2)$ symmetry. In section 6, a more complex system, $SU(3)$, is discussed. Finally we conclude in Section 7.

2. Geometry of the Phase Space

The construction of the classical limit for Lie algebras is opposite to the usual route taken to define the quantum theory. This is shown schematically in Table 1. If we start in an unconstrained phase space, the quantum limit can be defined by replacing Poisson brackets with commutation relations, replacing classical variables with quantum operators and adding an i appropriately (we set $\hbar = 1$). This prescription can be followed for the canonical commutation relations as well as the equations of motion, now in the Heisenberg picture. The classical theory is in some sense more general, as we can compute the Poisson bracket of arbitrary functions, whereas the commutation relations of arbitrary functions are not generally easy to evaluate. Also the classical theory has a wider class of symmetries realized in terms of (nonlinear) canonical transformations. When we come to Lie algebras, we have an apriori quantum theory. What we would like to do is produce a corresponding classical theory, developing all the structure from the Poisson brackets. In this section we review aspects of the classical limit of Lie algebras [10] . The classical limit corresponds to a classical theory completely analogous to the usual quantum theory. We begin with a set of N generators and commutation relations defining a Lie algebra

$$\left[\hat{X}_i, \hat{X}_j\right] = ic_{ijk}\hat{X}_k, \qquad (i,j,k = 1,...,N), \tag{2.1}$$

where c_{ijk} is totally antisymmetric. In the classical limit the generators pass to classical coordinates (c-numbers) which define an N dimensional Euclidian space. For arbitrary functions $\mathcal{F}(X)$ and $\mathcal{G}(X)$ over this space, the Poisson structure of the classical limit of Lie algebras is then defined through the Lie-Poisson brackets [14]

$$\{\mathcal{F}(X), \mathcal{G}(X)\} = \frac{\partial \mathcal{F}}{\partial X_i}\frac{\partial \mathcal{G}}{\partial X_j}c_{ijk}X_k = G_{ij}(X)\frac{\partial \mathcal{F}}{\partial X_i}\frac{\partial \mathcal{G}}{\partial X_j}. \tag{2.2}$$

Here $G_{ij}(X)$ is the antisymmetric Poisson tensor, which explicitly dependends

TABLE 1. Transition between classical and quantum mechanics

Classical		Quantum
$\{q_i, p_j\} = \delta_{ij}$	$\longrightarrow$	$[\hat{q}_i, \hat{p}_j] = i\delta_{ij}$
Equations of Motion :		
$\frac{\partial q_k}{\partial t} = \{q_k, H\} = \frac{\partial H}{\partial p_k}$		$i\frac{\partial \hat{q}_k}{\partial t} = \left[\hat{q}_k, \hat{H}\right]$
$\frac{\partial p_k}{\partial t} = \{p_k, H\} = -\frac{\partial H}{\partial q_k}$	$\longrightarrow$	$i\frac{\partial \hat{p}_k}{\partial t} = \left[\hat{p}_k, \hat{H}\right]$
$\frac{\partial F}{\partial t} = \{F, H\}$		$i\frac{\partial \hat{F}}{\partial t} = \left[\hat{F}, \hat{H}\right]$
General Functions :		
$\{F, G\} = \frac{\partial F}{\partial q_k}\frac{\partial G}{\partial p_k} - \frac{\partial F}{\partial p_k}\frac{\partial G}{\partial q_k}$	$\longrightarrow$	$\left[\hat{F}, \hat{G}\right]$
Lie Algebra :		
?	$\longleftarrow$	$\left[\hat{X}_i, \hat{X}_j\right] = ic_{ij}^k \hat{X}_k$

on the (non-canonical) coordinates X. The parallel between the quantum and classical limits is apparent if we take $\mathcal{F}(X) = X_i$ and $\mathcal{G}(X) = X_j$, in which case

$$\{X_i, X_j\} = c_{ijk}X_k = G_{ij}(X) = -G_{ji}(X). \tag{2.3}$$

A general feature of rank n Lie algebras is the existence of n Casimir operators $(\hat{C}^1, ..., \hat{C}^n)$, as indicated in Table 2. These operators are polynomial functions of the generators which commute with all the generators:

$$\left[\hat{C}^\alpha, \hat{X}_j\right] = 0, \qquad (\alpha = 1, ..., n;\ j = 1, ..., N). \tag{2.4}$$

Since Eq. (2.4) is a property of the commutation relations (2.1), and in view of the classical parallel (2.3) , it is clear that in general we have the analogous relation at the classical level:

$$\{C^\alpha, X_j\} = 0, \qquad (\alpha = 1, ..., n;\ j = 1, ..., N), \tag{2.5}$$

where C^α are polynomial functions in the Euclidian coordinates X_k. Since these functions C^α have zero Lie-Poisson bracket with each X_j, it follows that they also have zero Lie-Poisson bracket with an arbirary Hamiltonian, in direct analogy with Dirac brackets.

TABLE 2. Number of canonical coordinates and invariants for the classical Lie algebras.

Lie Algebra	Number of Casimirs	Polynomial Order of Casimirs	Number of Pairs (q,p)
$SU(n)$	$n-1$	$C_2, C_3, \ldots, C_n$	$\frac{n(n-1)}{2}$
$SO(2n)$	n	$C_2, C_4, \ldots, C_{2n-2}, C_n$	$n(n-1)$
$SO(2n+1)$	n	$C_2, C_4, \ldots, C_{2n}$	n^2
$Sp(2n)$	n	$C_2, C_4, \ldots, C_{2n}$	n^2
G_2	2	C_2, C_6	6
F_4	4	C_2, C_6, C_8, C_{12}	24
E_6	6	$C_2, C_5, C_6, C_8, C_9, C_{12}$	36
E_7	7	$C_2, C_6, C_8, C_{10}, C_{12}, C_{14}, C_{18}$	63
E_8	8	$C_2, C_8, C_{12}, C_{14}, C_{18}, C_{20}, C_{24}, C_{30}$	120

Due to the existence of the n Casimir constraints, or constants of the motion, any trajectory is confined to a compact $(N-n)$ dimensional manifold $\mathcal{M}$ embedded in R^N and parametrized by N non-canonical coordinates X_i $(i = 1, ..., N)$. It is not possible to globally define a set of coordinates and momenta on these manifolds, although all the usual classical invariants, such as the symplectic 2-form $dp \wedge dq$, can be constructed in terms of the coordinates X_i [10] . Nevertheless, the geometry can be defined through the gradients of the Casimir functions $C^\alpha(X)$, which are normal to the phase space manifold $\mathcal{M}$. Aside from special cases, which we do not consider here, these gradients are linearly independent and span the n dimensional space normal to the phase space. It is convenient to define n orthonormal vectors $\hat{e}^\alpha$, related to the gradients through a linear transformation M:

$$\begin{pmatrix} \nabla C^1 \\ \vdots \\ \nabla C^n \end{pmatrix} = M \begin{pmatrix} \hat{e}^1 \\ \vdots \\ \hat{e}^n \end{pmatrix} . \tag{2.6}$$

The unit vectors e_i^α are labeled with greek superscripts $(\alpha, \beta, ...)$, and their components in R^N are labeled with roman subscripts $(i, j, ...)$. These vectors form a orthonormal basis for the n dimensional space normal to the $N-n$ dimensional phase space manifold $\mathcal{M}$. (These vectors are convenient at the formal level. However, the equations of motion we obtain are independent of them.) The case of $SU(2)$ provides a simple illustration and is good to keep in mind. Since there

are three generators (J_x, J_y, J_z), $N = 3$. The conserved quantity is the angular momentum J^2, or the radius of the sphere. In this case the $N - 1 = 2$ dimensional space is the surface of the 2-sphere S^2, and the $n = 1$ dimensional space is the radial direction, normal to the surface of the sphere, and in the direction of $\nabla J^2 \propto \hat{\mathbf{J}}$.

In the forthcoming discussion, we will need to define a generalized Liouville continuity equation on this compact phase space manifold, for which we will require derivatives on the phase space. The unit vectors defined in Eq. (2.6) allow a convenient definition of this phase space derivative:

$$\frac{D}{DX_i} = \nabla_i - \sum_{\alpha=1}^{n} e_i^\alpha (\hat{e}^\alpha \cdot \nabla). \tag{2.7}$$

When applied to the Casimir functions, this derivative is vanishing by construction, since it projects the usual Euclidian gradient ∇ onto the phase space by subtracting the components normal to the phase space manifold. It should be clear that the inner product of this derivative with any vector normal to the phase space is by definition a null operator:

$$\sum_{k=1}^{N} e_k^\alpha \frac{D(\cdots)}{DX_k} \equiv 0, \qquad (\alpha = 1, ..., n). \tag{2.8}$$

We will also need to construct general vector fields that are orthogonal to the gradients of the Casimir functions. There are many ways to generate these types of vector fields. For example, one can take a general N dimensional vector field $A_k(X)$ and project in onto the $N - n$ dimensional phase space manifold $\mathcal{M}$:

$$A_k^{\shortparallel}(X) = A_k(X) - \sum_{\alpha=1}^{n} e_k^\alpha (A \cdot \hat{e}^\alpha). \qquad \text{(projected)} \tag{2.9a}$$

Alternately, the structure constant can be used to project onto $\mathcal{M}$ as well. This method is similar to a generalized cross-product since it adds a twist to the projection above:

$$A_k^{\shortparallel}(X) = c_{ijk} A_j(X) X_k = G_{ij} A_j(X). \qquad \text{(twisted)} \tag{2.9b}$$

(The sum over repeated indices is implied throughout this article.) The fact that this projection is not unique is unessential for the method we are going to describe. Other projection schemes can also be implemented, although the

twisted method seems to be the simplest one. In either case, the resulting vector field is in the tangent to the phase space manifold:

$$\nabla C^\alpha \cdot A^{||} = 0, \qquad \text{or} \qquad \hat{e}^\alpha \cdot A^{||} = 0. \tag{2.10}$$

We shall establish now a series of formal identities, needed in Section 4. The reader can skip this part at the first reading and return to it when refered later on. Since the Hamiltonian flow from the Lie-Poisson brackets is restricted to the phase space manifold, the derivative (2.7) acting on the Lie-Poisson bracket is equivalent to the ordinary Euclidian gradient, and is identically zero by antisymmetry of the structure constants. To establish this

$$\frac{D}{DX_k}\{X_k, H(X)\} = \frac{\partial}{\partial X_k}\left(c_{klm}\frac{\partial H}{\partial X_l}X_m\right) - \sum_{\alpha=1}^{n} e_k^\alpha e_j^\alpha \frac{\partial}{\partial X_j}(c_{klm}X_m\frac{\partial H}{\partial X_l}). \tag{2.11}$$

The first term vanishes due to the antisymmetry of the structure constant. To see that the second term also vanishes, recall equation (2.5). In terms of components

$$0 = \{C^\alpha, \mathcal{F}(X)\} = c_{ijk}\frac{\partial C^\alpha}{\partial X_i}X_k\,\mathcal{G}_j(X), \tag{2.12}$$

where

$$\mathcal{G}_j(X) = \frac{\partial \mathcal{F}}{\partial X_j} \tag{2.13}$$

and $\mathcal{F}(X)$ is an arbitrary function of X. Equation (2.12) indicates that the structure constants contracted with any unit vector $\hat{e}^\alpha$ (recall that the gradients ∇C^α are expressible in terms of these unit vectors through the definition (2.6)) and coordinate X_k identically vanishes. Eq. (2.11) then reduces to

$$\frac{D}{DX_k}\{X_k, H(X)\} \equiv 0. \tag{2.14}$$

We also have trivially:

$$\frac{DX_i}{DX_i} = N - n. \tag{2.15}$$

In general, for computations which rely on the projections of Eq. (2.9a) , there will be the need to evaluate sums of the form

$$\frac{De_k^\alpha}{DX_k} = \frac{\partial e_k^\alpha}{\partial X_k} - \sum_\beta e_k^\beta e_l^\beta \frac{\partial e_k^\alpha}{\partial X_l}. \tag{2.16}$$

These derivatives will require knowledge of the unit vectors and must be constructed case by case.

We conclude with some final remarks on the classical limit of Lie algebras. The general field of geometric quantization deals with methods to determine the proper functions on classical phase space that can be realized in terms of quantum operators. That is, general classical functions of q_i and p_i do not always have corresponding quantum counterparts. The classic example is that of defining the proper quantum canonical coordinates on compact phase spaces, such as the torus $\{(q,p) \pmod 1\}$. In the classical limit of Lie algebras, the generators pass to classical coordinates, and the Casimir operators become classical functions that commute through the Lie-Poisson brackets irrespective of the Hamiltonian. At the same time this is equivalent to the fact that the Casimir function are all in involution [15] , i.e. they also commute among themselves as well. These Casimir functions are constants of motion that induce a topology on the phase space. The classical limit of the generators are non-canonical coordinates. As the phase space is compact, we cannot define canonical coordinates globally, and we are limited to local expressions of p and q in terms of the non-canonical generators. Due to the constraints, there are more generators X than coordinates and momenta (p,q). The advantage of begining with the quantum limit is now apparent. We know *apriori* exactly which functions of the classical (local) coordinates (p,q) correspond to quantum operators: it is precisely those combinations that produce the generators of the Lie algebra. In this way the formalism of geometric quantization can be completely circumvented.

3. Ergodicity

Consider a system evolving in time according to some Hamiltonian H, and an arbitrary observable $A(q,p)$. The dynamical equations of motion are given by the Poisson brackets, and have the form $\dot{\phi} = \mathcal{F}(\phi)$, where $\phi = (q_1, ..., p_N)$. It is natural to define the time average of $A(q,p)$ over the classical trajectory

$$\overline{A}(q,p) = \lim_{t\to\infty} \frac{1}{t} \int_0^t dt'\ A(q(t'),p(t')). \tag{3.1}$$

Such a trajectory is illustrated in Fig. 1 (left side). (It is allowed to cross over itself since it is projected onto the (q,p) space from a larger space.) The points indicate the time integrated solution to the equations of motion, and are separated by the integration time step. We can also define the phase space average of $A(q,p)$, given by

$$\langle A(q,p)\rangle = \frac{1}{Z} \int d\mu\ A(q,p). \tag{3.2}$$

Here $d\mu$ is the phase space measure, and Z is the normalization constant. Since

we are interested in the canonical ensemble average of $A(q,p)$, our measure will include a Boltzmann factor $\exp(-H/T)$. A system is then defined to be *ergodic*, in the sense of the *canonical ensemble*, if

$$\langle A(q,p)\rangle = \overline{A}(q,p), \tag{3.3}$$

except on a set of measure zero (usually denoted a.e. for almost everywhere.) This is illustrated in Fig. 1 (a-b). In this figure, the time average of A (Eq. (3.1)) along the classical trajectory is given by the summation of $A(q(t_i),p(t_i)) = A(q_i,p_i)$ evaluated at the points separated by dt, the integration time step, on the trajectory. If the phase space is partitioned into cells (right side of Fig. 1), these points can be binned into a histrogram, which generates a density distribution on the phase space. The time average of A is then equivalent to the phase space average of A weighted by this density distribution. An ergodic trajectory will reproduce the Boltzmann factor density in the phase space. (In the cases we consider below, we will use non-canonical coordinates together with constraints, which modifies the measure. The discussion in this section generalizes trivally to this case.) If the system is ergodic, these averages are *independent* of the initial conditions. This is an important requirement for convergence of the algorithm for a general Hamiltonian.

Another often encountered definition is *mixing*. A system is *mixing* if correlations vanish on long (possibly infinite) time scales. A system that is *mixing* is ergodic, but the converse is not always true.

4. Coupling to the Heat Bath

4.1. Equations of Motion

The Hamiltonian equations of motion on the compact phase space can be expressed in terms of the non-canonical coordinates through the Lie-Poisson brackets of Eq. (2.2):

$$\dot{X}_i = \{X_i, H\} = G_{ij}(X)\,\frac{\partial H}{\partial X_j}, \tag{4.1}$$

where the dot represents the time derivative, and the antisymmetric Poisson tensor has the form (for Lie algebras)

$$G_{ij}(X) = c_{ijk}X_k. \tag{4.2}$$

In the treatment of unconstrained classical systems in I, heat bath couplings were explicitly added to each of Hamiltons equation of motion. For constrained

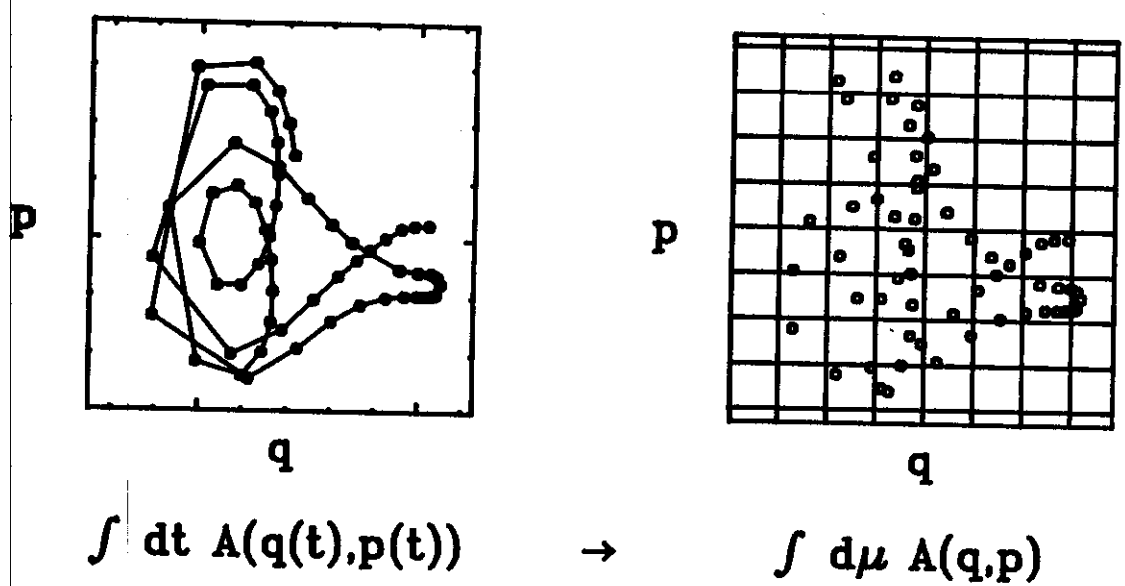

FIGURE 1. Relation between time average and phase space average for simulations of ergodic equations of motion.

systems, the coupling of these degrees of freedom to a heat bath can be achieved through the introduction of an arbitrary vector field $A_k^{\|}(X)$ tangent to the phase space, and a heat bath coupling $g(\zeta)$ (or pseudofriction):

$$\dot{X}_i = \{X_i, H\} - g(\zeta) A_i^{\|}. \tag{4.3}$$

By choosing projected or twisted forms of $A^{\|}$, one has the following equations of motion:

$$\dot{X}_i = G_{ij}\frac{\partial H}{\partial X_j} - g(\zeta)\left(A_k - \sum_{\alpha=1}^{n} e_k{}^{\alpha}(A\cdot\hat{e}^{\alpha})\right), \qquad \text{(projected)} \tag{4.3a}$$

$$\dot{X}_i = G_{ij}\left\{\frac{\partial H}{\partial X_j} - g(\zeta)A_j\right\}. \qquad \text{(twisted)} \tag{4.3b}$$

Here the pseudofriction function $g(\zeta)$ is an arbitrary function, coupled to the projection of an arbitrary vector field $A_k(X)$ in order to to ensure that all the constraints are preserved throughout the time evolution. We will limit the discussion in this section to only one pseudofriction function, although in principle there is no restriction on their number, and the formalism is trivially extended.

In general, we do not simply want to redefine the Hamiltonian. Rather, we want to violate phase space volume conservation. This is in complete analogy with the unconstrained case, see I, where we had to break the symplectic structure of the equations of motion in order to describe the effect of the thermostat on the system in question. We require that

$$\frac{\partial \dot{X}_i}{\partial X_i} = g(\zeta) G_{ji}\partial_i A_j \neq 0. \tag{4.4}$$

Having defined an $N+1$ dimensional extended space (X,ζ), an extended space probability distribution $f(X,\zeta)$ can be introduced. A natural choice of f is

$$f(X,\zeta) = \mathcal{N}\exp\left(-\frac{1}{T}\left\{H(X) + \frac{1}{\alpha}G(\zeta)\right\}\right). \tag{4.5}$$

Here α is a free parameter, which controls the rate at which the energy is exchanged between the envisaged system and the thermostat, $H(X)$ is the Hamiltonian of the envisaged system, T is the temperature and $\mathcal{N}$ a normalization constant. The function $G(\zeta)$ is an arbitrary function, the only restriction being

that f is normalizable. The extended space density f defines the measure on $\mathcal{M}$, or equivalently, the (generalized) canonical ensemble:

$$\langle\langle(\cdots)\rangle\rangle = \frac{1}{Z}\int d\mu(\cdots) = \frac{1}{Z}\int f\, d\zeta \prod_{i=1}^{N} dX_i \prod_{\alpha=1}^{n} \delta(C^\alpha - C_0^\alpha)(\cdots). \tag{4.6}$$

Here C_0^α are the values of the constraints (constants of motion) C^α, which are defined by the initial conditions, and $Z = \int d\mu$ is the partition function. If a system is ergodic, then the time average of any operator in the extended space $A(X,\zeta)$ is independent of initial conditions and the canonical ensemble average is obtained from the time average:

$$\lim_{t\to\infty} \frac{1}{t}\int_0^t dt'\; A(X(t'),\zeta(t')) = \frac{1}{Z}\int d\mu\; A(X,\zeta). \tag{4.7}$$

In the equations of motion (4.3a) - (4.3b) , we have explicitly extended the classical phase space by one degree of freedom, ζ. In adding the coupling to ζ, the Poisson structure of the equations of motion has been broken : Eqs. (4.3a) - (4.3b) are no longer in the form of Eq. (4.1). If we could define the coordinates q and momenta p in terms of the generators X, this is equivalent to saying that the conventional Liouville equation in q and p is violated. In order to discuss conservative time evolution of probability distribution $f(X,\zeta)$, we must define a Liouville continuity equation in terms of the non-canonical variables X and the heat bath degrees of freedom ζ. This equation must restrict the flow to the phase space manifold. A suitable choice is the following:

$$0 = \frac{\partial f}{\partial t} + \sum_{i=1}^{N} \frac{D(f\dot{X}_i)}{DX_i} + \frac{\partial(f\dot{\zeta})}{\partial\zeta}. \tag{4.8}$$

The derivative D, defined in Eq. (2.7), ensures that the flow of Eqs. (4.3a) - (4.3b) is in the phase space manifold $\mathcal{M}$, whereas the ζ direction is unrestricted in this sense. Let us summarize the steps up to this point. We have introduced augmented equations of motion (4.3a) - (4.3b) , a postulated phase space density (4.5) and a generalized Liouville equation on this extended space (4.8). In order to make these consistent, (4.3a) or (4.3b) and (4.5) can be inserted into the Liouville equation and an equation of motion derived for ζ. In general this results in a self-consisent differential equation that must be solved. One solution is easily

obtained if we start with the ansatz

$$\frac{d\dot{\zeta}}{d\zeta} = 0. \tag{4.9}$$

Solving the Liouville equation we obtain the equation of motion for ζ:

$$\dot{\zeta} = \alpha \left[\frac{g}{dG/d\zeta}\right] \left(A^{\|} \cdot \nabla H - T\frac{DA_k^{\|}}{DX_k}\right), \qquad \text{(projected)} \tag{4.10a}$$

$$\dot{\zeta} = \alpha c_{ijk} X_k \left[\frac{g}{dG/d\zeta}\right] \left(A_j \frac{\partial H}{\partial X_i} - T\frac{\partial A_j}{\partial X_i}\right). \qquad \text{(twisted)} \tag{4.10b}$$

The results in Eq. (4.10b) are obtained when one realizes that $e_i^{\alpha} c_{ijk} X_k \equiv 0$, which comes from Eq. (2.12). We have detailed the derivation in the appendix. The condition (4.9) together with the equation of motion (4.10a) or (4.10b) result in the consistency condition that the term in the square brackets must be independent of ζ. By absorbing any constants into the definition of α, we set

$$g(\zeta) \equiv \frac{dG}{d\zeta}. \tag{4.11}$$

Thus, the choice of $g(\zeta)$ in the equations of motion determines the thermal distribution of ζ in the canonical ensemble. The resulting equations of motion, which by construction preserve the extended space density f during time evolution, are hence forth given by:

Projected :

$$\begin{aligned} \dot{X}_i &= c_{ijk}\frac{\partial H}{\partial X_j} X_k - g(\zeta)\left(A_k - \sum_{\alpha=1}^{n} e_k{}^{\alpha}(A \cdot \hat{e}^{\alpha})\right), \\ \dot{\zeta} &= \alpha\left(A^{\|} \cdot \nabla H - T\frac{DA_k^{\|}}{DX_k}\right), \end{aligned} \tag{4.12}$$

Twisted :

$$\begin{aligned} \dot{X}_i &= c_{ijk} X_k \left(\frac{\partial H}{\partial X_j} - g(\zeta) A_j\right), \\ \dot{\zeta} &= \alpha c_{ijk} X_k \left(A_j \frac{\partial H}{\partial X_i} - T\frac{\partial A_j}{\partial X_i}\right). \end{aligned} \tag{4.13}$$

In this form the pseudofriction ζ couples to all degrees of freedom. This not neccesary and other types of coupling can be introduced as well if needed. In

practice, the method using the twisted projection provides a much simpler prescription for coupling the system to the heat bath since it does not require any knowledge of the unit vectors $\hat{e}^\alpha$. In the applications below, we will consider both methods. In general, additional pseudofriction couplings can be added to the equations of motion (4.12)-(4.13) in the form $g'(\xi)B_k^{\|}$ and to the distribution function f in eq. (4.5) in the form $G'(\xi)/\beta$. The resulting equation for $\dot{\xi}$ is precisely analogous to that one for $\dot{\zeta}$, with α, A_k and ζ replaced by β, B_k and ξ, respectively. In practice it seems that one pseudofriction is not enough to generate ergodic trajectories, and two is a minimum number.

Finally, we observe that there is a quantity conserved by the equations of motion, denoted the pseudo-energy:

$$\mathcal{E} = H(X) + \frac{1}{\alpha}G(\zeta) + T\int dt' g(\zeta)\frac{\partial A_k^{\|}}{\partial X_k}. \tag{4.14}$$

By direct substitution of the equations of motion into $\dot{\mathcal{E}}$ it is easily checked that $\dot{\mathcal{E}} = 0$. The term inside the integral corresponds to the divergence of the equations of motion (4.4).

4.2. Stability

Although the equations of motion (4.12)-(4.13) are consistent with the thermal distribution and Liouville equation, there is no guarantee that the functions $g(\zeta)$ and $A_k(X)$ lead to ergodic trajectories. Since we will primarily study the twisted equations of motion (4.13), it should be demonstrated that at least there are no stable fixed points in those equations of motion. This can be acheived by linearizing the equations of motion around an arbitrary point in the extended space and studying the eigenvalue problem of the resulting stability matrix. We will take a case where there are two pseudofriction functions, although the argument holds for any number of them. By defining the vector

$$\phi = (X_1, ..., X_N, \zeta, \xi), \tag{4.15}$$

the equations of motion (4.13) can be written as

$$\dot{\phi} = \mathcal{F}(\phi). \tag{4.16}$$

Linearizing around an arbitrary point in the extended space ϕ_0, defines the sta-

bility matrix:

$$\dot{\phi} = \left(\frac{\partial \mathcal{F}_i}{\partial \phi_j}\right)_{\phi_0} \phi_j. \tag{4.17}$$

The sum of the eigenvalues of the stability matrix is given by its trace:

$$\mathrm{Tr}\left(\frac{\partial \mathcal{F}_i}{\partial \phi_j}\right)_{\phi_0} = \sum_i \lambda_i = g(\zeta) c_{ijk} X_k \frac{\partial A_j}{\partial X_i} + h(\xi) c_{ijk} X_k \frac{\partial B_j}{\partial X_i}. \tag{4.18}$$

The fixed point (FP) condition is $\dot{\phi} = 0$, which leads to the conditions

$$\begin{aligned} c_{ijk} X_k \frac{\partial H}{\partial X_j} &= g(\zeta) c_{ijk} X_k A_j + h(\xi) c_{ijk} X_k B_j, \\ c_{ijk} X_k A_j \frac{\partial H}{\partial X_i} &= T c_{ijk} X_k \frac{\partial A_j}{\partial X_i}, \\ c_{ijk} X_k B_j \frac{\partial H}{\partial X_i} &= T c_{ijk} X_k \frac{\partial B_j}{\partial X_i}. \end{aligned} \tag{4.19}$$

The r.h.s of the last two conditions can be inserted into the trace formula (4.18):

$$\mathrm{Tr}\left(\frac{\partial \mathcal{F}_i}{\partial \phi_j}\right)_{\phi_0} = \frac{1}{T} c_{ijk} X_k \left[g(\zeta) A_j \frac{\partial H}{\partial X_i} + h(\xi) B_j \frac{\partial H}{\partial X_i} \right]. \tag{4.20}$$

Using the r.h.s. of the first condition in (4.19), we have

$$\mathrm{Tr}\left(\frac{\partial \mathcal{F}_i}{\partial \phi_j}\right)_{\phi_0} = \sum_i \lambda_i = \frac{1}{T} c_{ijk} X_k \frac{\partial H}{\partial X_i} \frac{\partial H}{\partial X_j} \equiv 0. \tag{4.21}$$

A stable fix point would correspond to negative values for all eigenvalues λ_i's. Hence there are no stable fixed points at finite temperature for any nontrivial choice of functions A, B, g and h. (An analogous treatment for the projected method is not simple, and it must be considered case by case.) This, together with comparison of the results of the method for several initial conditions is in practice sufficient to determine ergodicity.

5. Hamiltonians with $SU(2)$ Symmetry

The simplest algebraic systems to study are Hamiltonians that can be expressed in terms of generators of $SU(2)$. For this case the (compact) phase space is the two-sphere S^2.

5.1. Equations of Motion

The quantum description for $SU(2)$ consists of the commutation relations

$$[\hat{J}_i, \hat{J}_j] = i\epsilon_{ijk}\hat{J}_k, \qquad (i,j,k = 1,2,3) \tag{5.1}$$

where ϵ_{ijk} is the Levi-Civita tensor. These commutation relations have the property that $\hat{J}^2 = \hat{J}_x^2 + \hat{J}_y^2 + \hat{J}_z^2$ commutes with any function of $\hat{J}_k$. In the classical limit for $SU(2)$, the J_i are classical coordinates and the symplectic structure of the classical phase space is defined by the Lie-Poisson brackets for arbitrary functions of J_k:

$$\{\mathcal{F}(J), \mathcal{G}(J)\} = \frac{\partial \mathcal{F}}{\partial J_i}\frac{\partial \mathcal{G}}{\partial J_j}\epsilon_{ijk}J_k. \tag{5.2}$$

The equations of motion for the coordinates can now be obtained using the Hamilton's equations of motion:

$$\dot{J}_i = \{J_i, H\} = \epsilon_{ijk}\frac{\partial H}{\partial J_j}J_k \tag{5.3}$$

In this section we consider the effects of two pseudofriction couplings using pseudofriction coefficients ζ and ξ. The most general equations of motion that we consider for an $SU(2)$ Hamiltonian H coupled to a heat bath using the twisted projection method are of the form:

$$\begin{aligned}
\dot{J}_i &= \{J_i, H\} - g_1(\zeta)A_i^{\|} - g_2(\xi)B_i^{\|} \\
&= \epsilon_{ijk}J_k\left(\frac{\partial H}{\partial J_j} - g_1(\zeta)A_j - g_2(\xi)B_j\right), \\
\dot{\zeta} &= \alpha\epsilon_{ijk}J_k\left(A_j\frac{\partial H}{\partial J_i} - T\frac{\partial A_j}{\partial J_i}\right), \\
\dot{\xi} &= \beta\epsilon_{ijk}J_k\left(B_j\frac{\partial H}{\partial J_i} - T\frac{\partial B_j}{\partial J_i}\right).
\end{aligned} \tag{5.4}$$

The pseudofriction terms g_1 and g_2 and the Hamiltonian define the canonical

ensemble through the phase space density

$$f(J,\zeta,\xi) = \exp\left(-\frac{1}{T}\left(H + \frac{1}{\alpha}G_1(\zeta) + \frac{1}{\beta}G_2(\xi)\right)\right), \tag{5.5}$$

where $g_1 = dG_1/d\zeta$ and $g_2 = dG_2/d\xi$. For arbitrary vector fields A_k and B_k it is easily verified that the Casimir function J^2 is preserved:

$$J_i \dot{J}_i \equiv 0. \tag{5.6}$$

We have studied the functions $g(\zeta)$ and $h(\xi)$ of the forms:

$$g_1(\zeta) = \begin{cases} \zeta^n, & n = 1,3; \\ \zeta|\zeta| \end{cases} \qquad g_2(\xi) = \begin{cases} \xi^n, & n = 1,3; \\ \xi|\xi| \end{cases} \tag{5.7}$$

For A and B we have chosen vectors that have nonzero curl. (In choosing the various functions, one must be careful not to allow stable fixed points in the equations of motion.) Some choices for the twisted case that lead to ergodic trajectories are:

$$A_k = (S_3, S_1, S_2), \quad B_k = (S_2, -S_1, 0), \quad C_k = (S_1S_2S_3, \sqrt{3}S_2S_3, \sqrt{5}S_1S_2) \tag{5.8}$$

When we use two pseudofrictions ($N = 2$), we refer to A and B, and all three for the $N = 3$ situation.

In studying the projected method, the equations of motion are somewhat longer:

$$\begin{aligned} \dot{J}_i &= \{J_i, H\} - g_1(\zeta)A_i^{\|} - g_2(\xi)B_i^{\|} \\ &= \epsilon_{ijk}\frac{\partial H}{\partial J_j}J_k - g_1(\zeta)\left[A_i - J_i\frac{A_mJ_m}{J^2}\right] - g_2(\xi)\left[B_i - J_i\frac{B_mJ_m}{J^2}\right], \\ \dot{\zeta} &= \alpha\left(A^{\|}\cdot\nabla H - T\frac{DA_k^{\|}}{DJ_k}\right), \\ \dot{\xi} &= \beta\left(B^{\|}\cdot\nabla H - T\frac{DB_k^{\|}}{DJ_k}\right). \end{aligned} \tag{5.9}$$

In this study we have taken $A_k(J) = \nabla_k a$ and $B_k(J) = \nabla_k b$ to be gradients of

polynomials $a(J)$ and $b(J)$ of the form:

$$a(J),\ b(J) = \sum_{i=1}^{3} \mu_i J_i + \sum_{i,j=1}^{3} \nu_{ij} J_i J_j, \tag{5.10}$$

where μ_i and ν_{ij} are constants. One suitable choice that we have found is

$$a(J) = \frac{1}{2}(J_2 - J_3)^2, \qquad b(J) = \frac{1}{4}(\sqrt{3}J_1 + J_3)^2. \tag{5.11}$$

5.2. Flat Space Analog

A direct comparison of these methods for compact spaces to the previous unconstrained (flat-space) methods of I can be made if we expand the equations of motion locally in a tangent plane to the phase space. Consider the north pole (NP) of the sphere. At this point $J_1 = J_2 = 0$ and $J = J_3$, and the only non-zero Lie-Poisson bracket is

$$\left\{ \frac{J_1}{\sqrt{J}}, \frac{J_2}{\sqrt{J}} \right\} |_{NP} = 1, \tag{5.12}$$

for which we associate $q = J_1/\sqrt{J}$ and $p = J_2/\sqrt{J}$. The twisted equations of motion have the form (absorbing constants into the definition of A):

$$\begin{aligned} \dot{J}_x &= J\frac{\partial H}{\partial J_y} + J g_1(\zeta) A_y + J g_2(\xi) B_y, \\ \dot{J}_y &= -J\frac{\partial H}{\partial J_x} - J g_1(\zeta) A_x - J g_2(\xi) B_x, \end{aligned} \tag{5.13}$$

or equivalently :

$$\begin{aligned} \dot{q} &= \frac{\partial H}{\partial p} + g_1(\zeta) A_p + g_2(\xi) B_p, \\ \dot{p} &= -\frac{\partial H}{\partial q} - g_1(\zeta) A_q - g_2(\xi) B_p. \end{aligned} \tag{5.14}$$

Here $A_{p,q} = \sqrt{J} A_{x,y}$ and $B_{p,q} = \sqrt{J} B_{x,y}$. This should now be contrasted to the method used to couple unconstrained systems to a heat bath in I:

$$\begin{aligned} \dot{q} &= \frac{\partial H}{\partial p} + h(\zeta) F(q,p) \\ \dot{p} &= -\frac{\partial H}{\partial q} - g(\xi) G(q,p) \end{aligned} \tag{5.15}$$

Thus in every tangent plane, a suitable choice of the components of A, A_p and A_q, can be made so that the methods look identical. The Liouville equation on

the tangent space can also be simplified since the projective derivative (2.7) takes the form

$$\begin{aligned}\frac{D}{DX_i} &= \frac{\partial}{\partial J_i} - \frac{J_i}{J^2} J_j \frac{\partial}{\partial J_j} \\ &= (\frac{\partial}{\partial J_1}, \frac{\partial}{\partial J_2}, 0)\end{aligned} \tag{5.16}$$

Placing this expression into the Liouville equation (4.8) one obtains:

$$0 = \frac{\partial f}{\partial t} + \frac{\partial (f\dot{q})}{\partial q} + \frac{\partial (f\dot{p})}{\partial p} + \frac{\partial (f\dot{\zeta})}{\partial \zeta} \tag{5.17}$$

which again is precisely the Liouville equation used for unconstrained systems. This demonstrates the close parallel with the methods for unconstrained systems.

5.3. Phase Space

In practice these techniques are simple to use. Consider the case of the classical rotor

$$H = \frac{\kappa}{2} J_3^2. \tag{5.18}$$

Using the twisted method (5.4) and the functions (5.8) we have the equations of motion

$$\begin{aligned}\dot{J}_1 &= -\kappa J_2 J_3 - \zeta J_1 J_3 + \xi^3 (J_1 J_3 - J_2^2), \\ \dot{J}_2 &= \kappa J_1 J_3 - \zeta J_2 J_3 + \xi^3 (J_1 J_2 - J_3^2), \\ \dot{J}_3 &= -\zeta (J_2^2 + J_3^2) + \xi^3 (J_2 J_3 - J_1^2), \\ \dot{\zeta} &= -\alpha J_3 (\kappa (J_2^2 + J_1^2) + 2T), \\ \dot{\xi} &= \beta (T(J_1 + J_2 + J_3) - \kappa J_3 (J_2 J_3 - J_1^2)).\end{aligned} \tag{5.19}$$

These equations of motion are evolved in time. A typical trajectory consisting of 5000 points, sampled every $dt = 0.02$ along the trajectory, is shown in Fig. 2. The initial condition used is

$$\phi = (J_1, J_2, J_3, \zeta, \xi) = (0, 0.555, -0.832, 0, 0) \tag{5.20}$$

together with $\alpha = \beta = T = 1$. In the numerical simulations, integration of the equations of motion was performed using the IMSL subroutine DIVPRK, with an error tolerance of $10^{-6} - 10^{-9}$. This routine is based on the programs of Hull, Enright and Jackson [17] , and uses Runge-Kutta formulas of order five and six, as cited in the IMSL User's manual. All computations were performed

in double precision on a VAX 3100 workstation, which has a 64-bit wordlength, in DEC VAX-FORTRAN. The dt referred to throughout the text is the sample time, which is in general larger than the actual integration step, determined by the subroutine. At every interval dt, various quantities, such as J_i, H and so forth, are sampled and binned. The resulting histrograms of these quantities correspond to the thermal distributions, which contain much more information than simply the moments or other averages. For example, by binning J_1, we obtain the thermal distribution $f(J_1)$. For the classical rotor (5.18), the exact results can also be obtained by direct integration in the canonical ensemble. Up to normalization, they are given by

$$\begin{aligned} f(J_1) &= \int dJ_2 dJ_3 e^{-\kappa J_3^2/2T} \delta(J_0 - J) \\ &= 2J\pi e^{-\kappa(J^2-J_1^2)/2T} I_0\left(\frac{\kappa(J^2-J_1^2)}{2T}\right), \\ f(J_2) &= 2J\pi e^{-\kappa(J^2-J_2^2)/2T} I_0\left(\frac{\kappa(J^2-J_2^2)}{2T}\right), \\ f(J_3) &= e^{-\kappa J_3^2/2T}, \end{aligned} \tag{5.21}$$

where I_0 is the Bessel function of the first kind. The thermal distributions corresponding to the trajectory in Fig. 2, obtained by binning at each sample time, is compared to the exact results (5.21) in Fig. 3. For a larger number of steps, the convergence improves considerably, as shown in Fig. 4. As we shall discuss below, convergence to the exact result generally behaves as $1/\sqrt{N}$, where N is the number of steps.

5.4. Convergence and Ergodicity

An important question is that of ergodicity. If the equations are ergodic, then the results obtained when using this method are independent of initial conditions, a property which is essential in order for this method to be of value. Unfortunately we are not aware of any methods to determine whether or not a general set of (non-Hamiltonian) equations are ergodic or not. Rather we resort to a more direct way of testing this. By partitioning the extended space into a lattice, we can take each lattice site as an initial condition and evolve each trajectory to a fixed final time t. At this time, the thermal distributions of each of the extended space variables are compared to the exact distributions, through the quantity $\Delta(t)$:

$$\Delta(\phi_i, t) = 100 \int \mid f_{exact}(\phi_i) - f_{calc}(\phi_i, t) \mid \; d\phi_i, \tag{5.22}$$

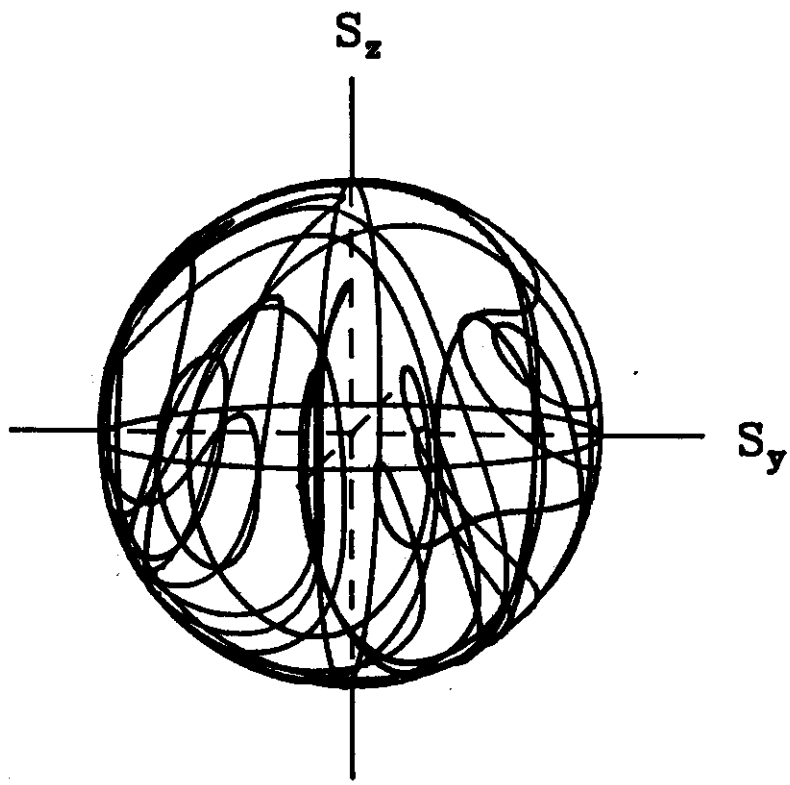

FIGURE 2. Ergodic trajectory on a sphere, evolved to a final time $t = 100$ using an integration time step $dt = 0.02$, for the classical rotor $H = J_z^2/2$.

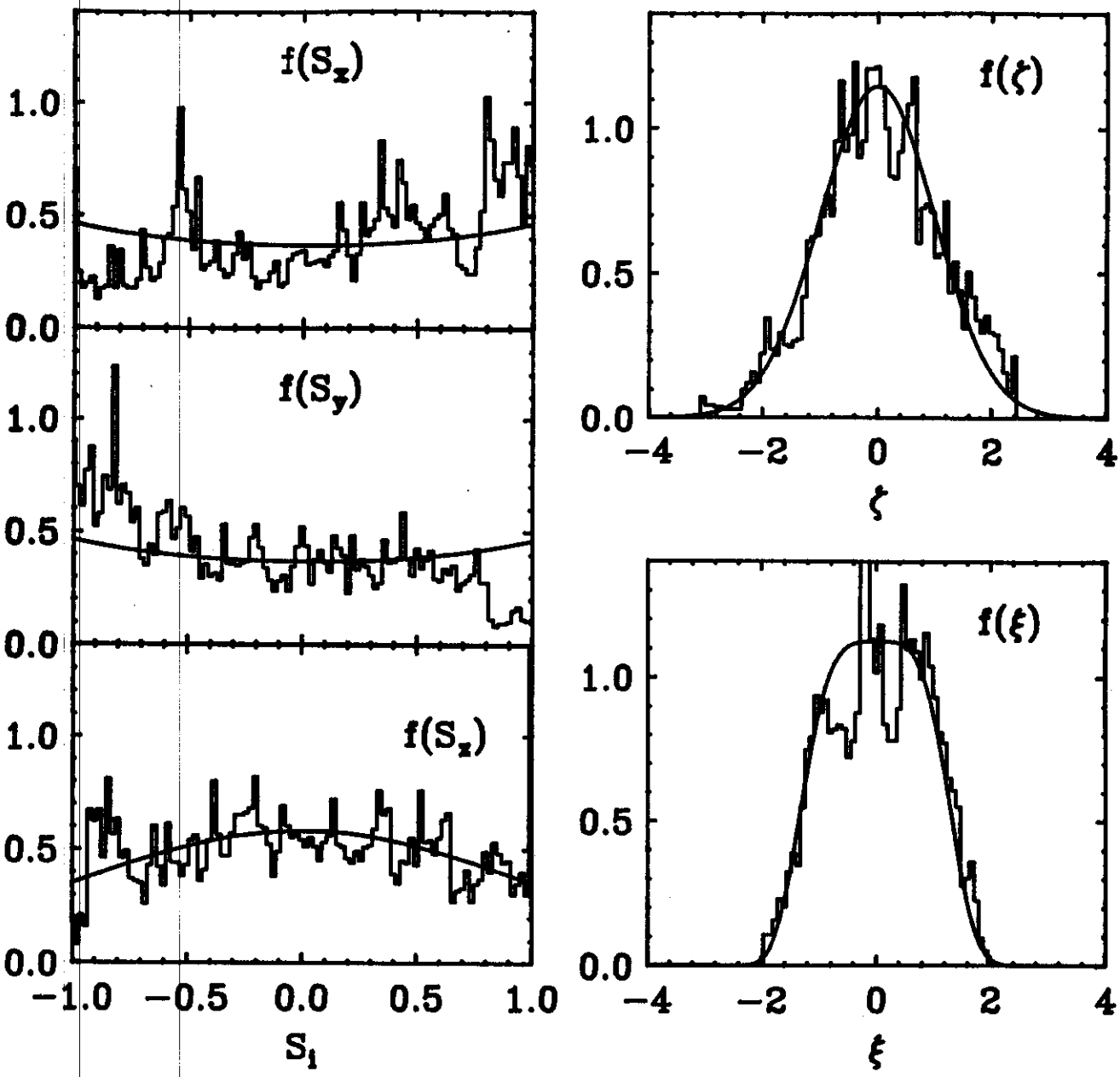

FIGURE 3. The thermal distributions corresponding to the trajectory in Fig. 2. already at this short time, the thermal distributions resemble to exact results.

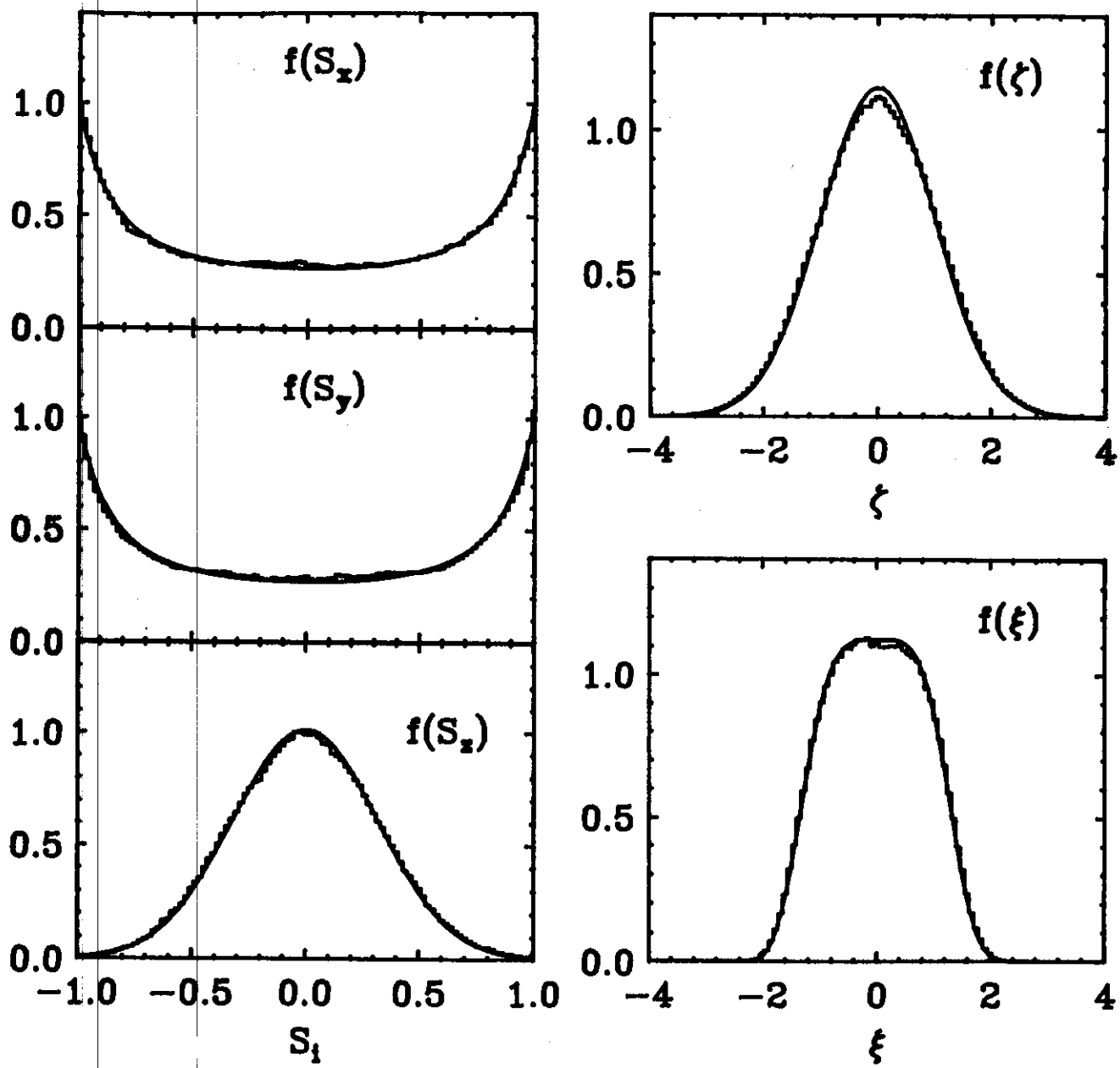

FIGURE 4. The same as Fig. 3, except a final time of $t = 30000$. The deviations from the exact result are statistical in origin.

which is defined as a percent deviation from the exact result. The distribution of the values of $\Delta(t)$ for each initial condition is an indication of ergodicity. If the results are similar for each initial condition, we take this as a practical test of ergodicity. (Recall, we have already chosen equations of motion with no stable fixed points.) In Fig. 5, we show the distributions of $\Delta(t = 100)$ obtained for 600 initial conditions, for the classical rotor $H = J_z^2/2$, using three pseudofrictions and the twisted method. For all the initial conditions, the deviations fall within a few percent of each other, indicating that the initial conditions are not important. Similar results can be obtained using the projected method.

Another quantity which is of interest is the rate of convergence to the canonical ensemble. This is obtained by studying the time evolution of $\Delta(t)$. In Fig. 6, we plot the time evolution $\Delta(t)$ for a classical rotor $H = J_z^2/2$ using the projected method. The dashed lines corresponds to $1/\sqrt{t} \propto 1/\sqrt{N}$, the statistical limit for convergence. Fig. 7 is identical to 6 except that we use the twited method, again with only two pseudofrictions. Obviously there is no significant difference between the methods for these cases, and the convergence has an average $1/\sqrt{N}$ behavior.

5.5. Lyapunov Exponents

The role of the pseudofriction terms is to create dynamical instabilities in the system of equations. A convenient tool for understanding the nature of the instability, is the Lyapunov exponents. These exponents measure the average exponential separation between two neighboring points in space. If we consider a small separation between two points in the extended space, represented by the vector ϵ, we can study the time evolution of ϵ over short times using the linearized equations of motion, introduced in section 4.2:

$$\dot{\epsilon}(t) = \frac{\partial \mathcal{F}}{\partial \phi}\epsilon(0). \tag{5.23}$$

Here $\dot{\phi} = \mathcal{F}(\phi)$ represent the equations of motion in the extended space. The formal solution is the time ordered integral

$$\epsilon(t) = \hat{T} \exp\left(\int_0^t dt' \frac{\partial \mathcal{F}}{\partial \phi}\right) \epsilon(0). \tag{5.24}$$

The maximum eigenvalue then has the form

$$\lambda_{max} = \lim_{n\to\infty} \frac{1}{n\,dt} \sum_{i=1}^{n} \log \mid \epsilon(i\,dt) \mid . \tag{5.25}$$

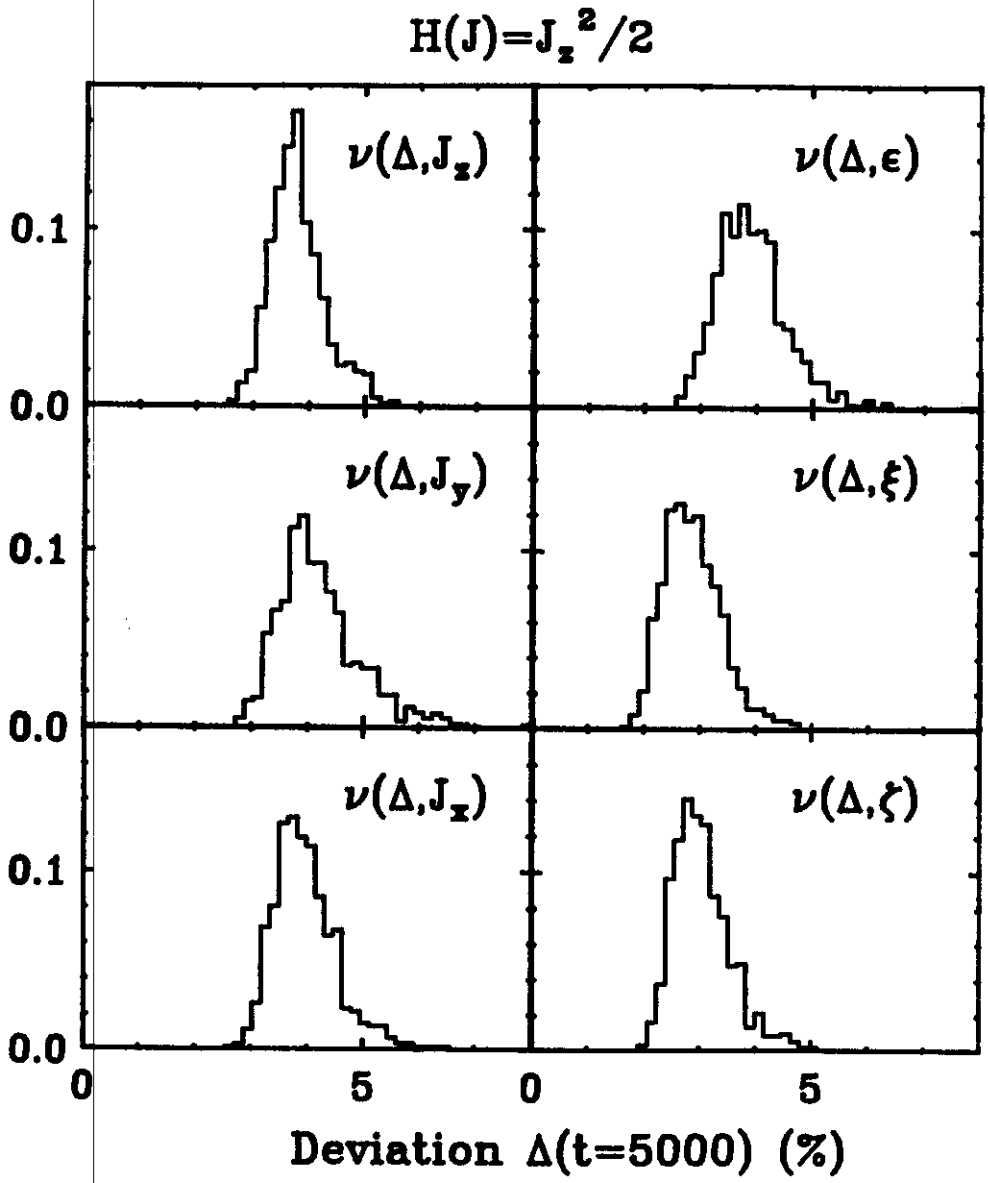

FIGURE 5. Normalized frequency distribution of the deviations $\Delta(\phi_i, t)$, for $t = 5000$, where $\phi = (J_1, J_2, J_3, \zeta, \xi, \epsilon)$. We have used three pseudofrictions on the classical rotor with the twisted method. The results are based on 600 initial conditions.

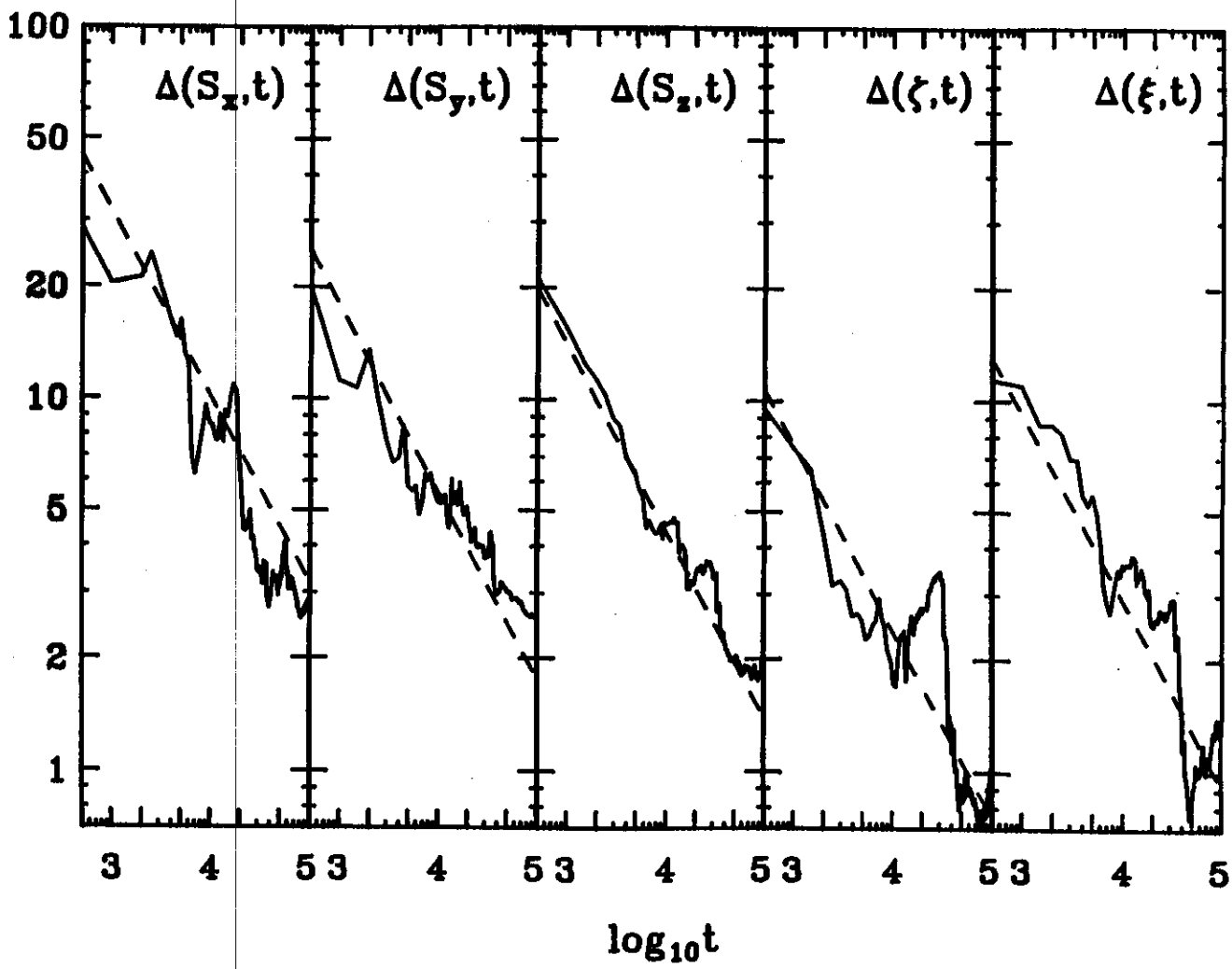

FIGURE 6. Rate of convergence of the relative deviations of the computed to the exact thermal distributions using the projected method with two pseudo-frictions for the classical rotor.

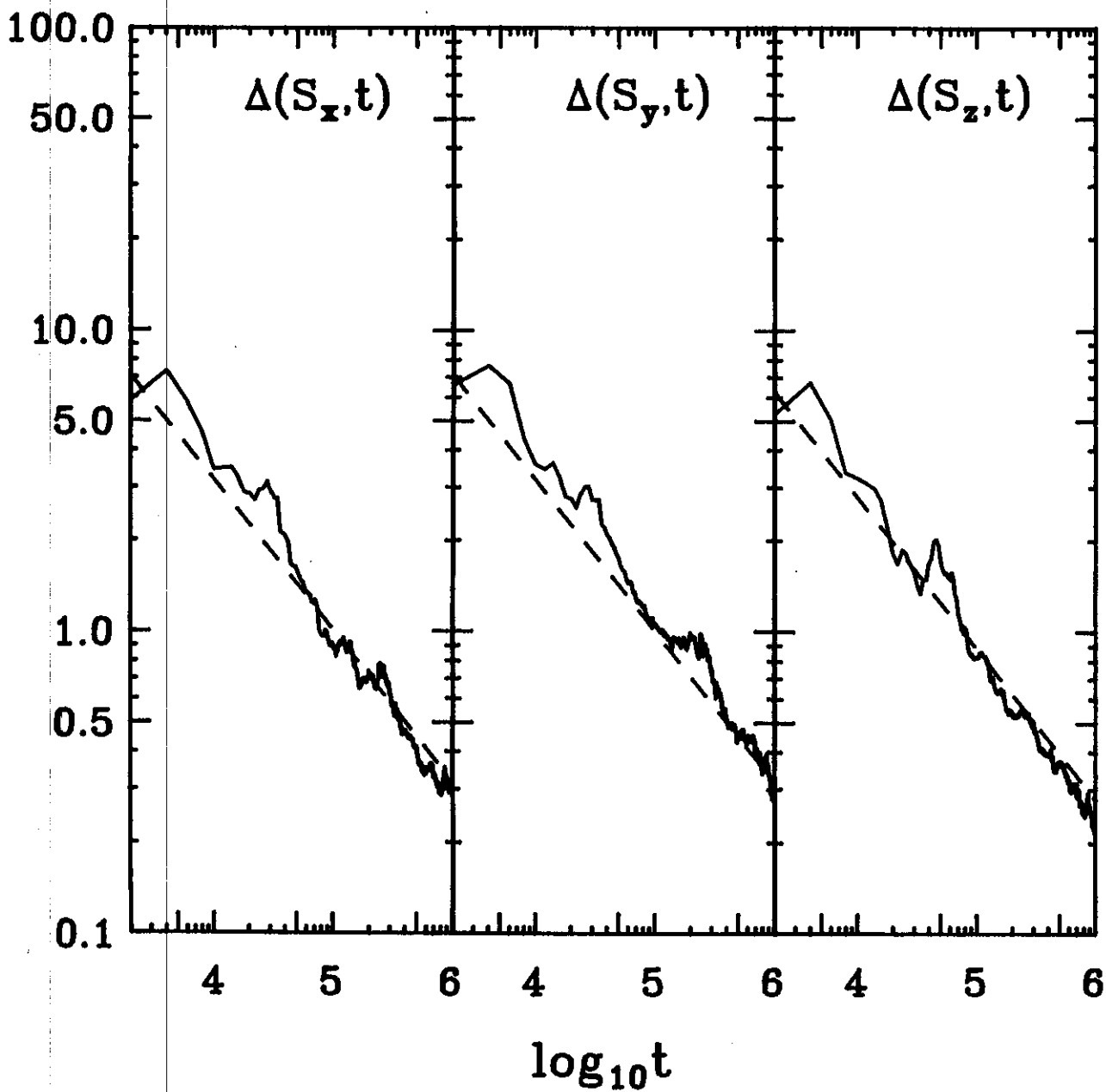

FIGURE 7. Same as Fig. 5, except using two pseudofrictions and the twisted method.

Typical exponents are shown in Fig. 8 for a classical rotor for selected values of α and β. These exponents have the same behavior observed in I for uncostrained dynamical systems: they are monotonically increasing functions of the coupling strengths α and β.

5.6. Mixing

An important property of these methods is the strength with which the pseudofrictions couple to all the degrees of freedom. This allows for rapid diffusion across the phase space. This can be illustrated with the classical rotor $H = J_z^2/2$. The extended space is projected onto phase space, which is the sphere S^2. A circle is defined on S^2 with $J_z = 0.5$ consisting of 10^3 points. Each of these points is taken as the initial condition, and evolved in time using the projected equations of motion. The characteristic time of the system is of order unity. The initial condition of the circle is plotted at $t = 0$ in Fig. 9. The same circle at later times $t = 10, 20$ and $t = 30$ is also shown in the figure. After only 20 cycles, the circle already covers the entire sphere. It is clear that the points diffuse across the phase space quite rapidly. This can be an important feature when studying systems close to a phase transition, where one has critical slowing down.

5.7. Correlations

Since the equations of motion are dynamical trajectories, it is possible to evaluate auto-correlation functions for the systems under study. Auto-correlation functions are shown in Figs. 10-11 for a classical rotor, using 2 and 3 pseudofrictions in the twisted scheme, and 2 pseudofrictions in the projected scheme. All auto-correlation functions have been normalized to unity at $\tau = 0$. It is clear that there is a strong dependence on the scheme one uses and on the choice of pseudofriction couplings. This is an essential feature, since the coupling of a system to a heat bath can depend on many parameters, such as the rate of exchange of heat, the type of coupling and so forth. This type of method has the potential to describe a wide variety of physical situations.

5.8. Spin Systems

The extension of the methods in the previous section to systems of coupled spins is straight forward. Consider for example the case of 50 spins on a periodic chain. The interaction is taken as a nearest neighbor anti-ferromagnetic

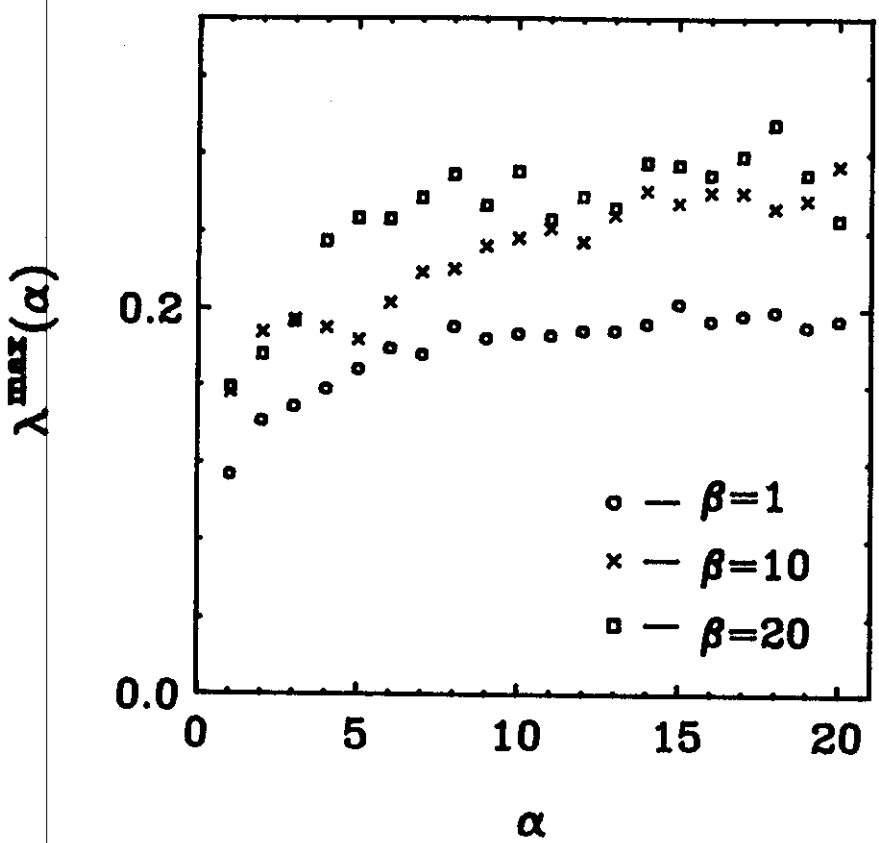

FIGURE 8. Behavior of the maximum Lyapunov exponent as a function of the coupling strenghts α and β.

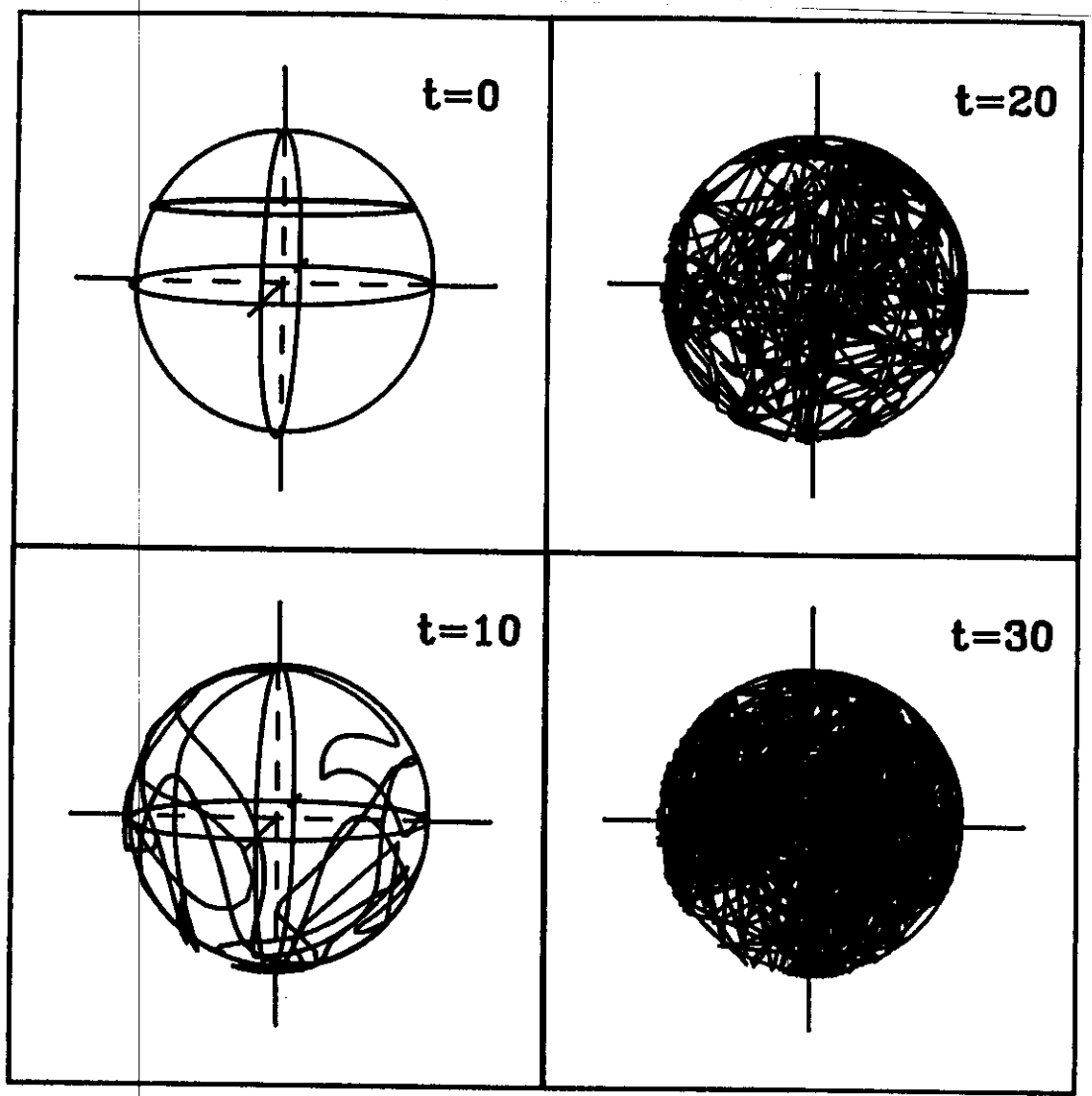

FIGURE 9. Time evolution of a circle, defined by 10^3 point, at $J_z = 0.5$. Each point is taken as an initial condition for a trajectory. The equations of motion are that of the classical rotor using the twisted method. The characteristic time of the system is $t \sim 1$. The structure of the circle is shown at times $t = 10, 20, 30$, indicating rapid spreading of points across phase space.

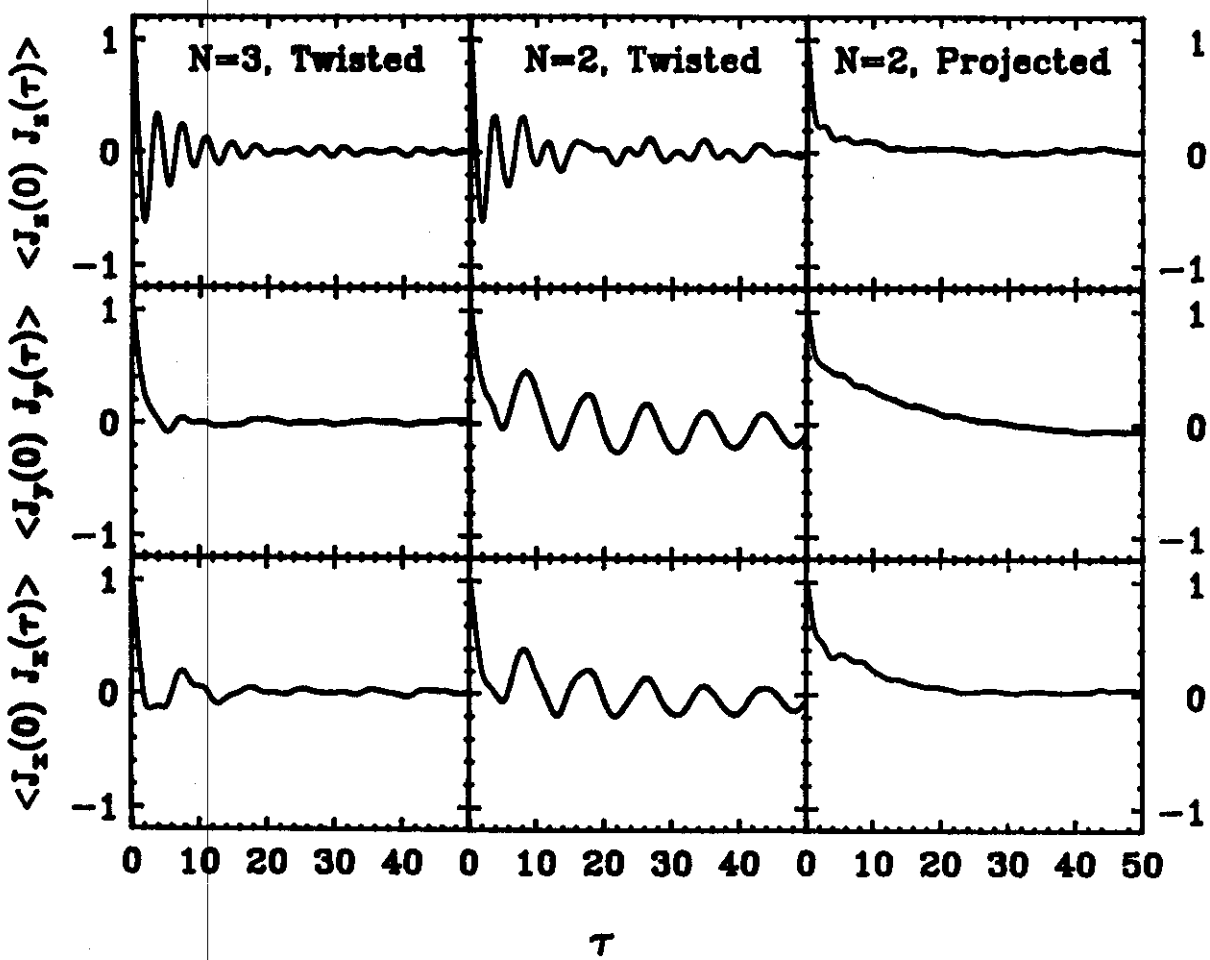

FIGURE 10. Comparison of spin auto-correlation functions for the classical rotor using twisted method with 2 and 3 pseudofrictions, and the projected method with two pseudofrictions.

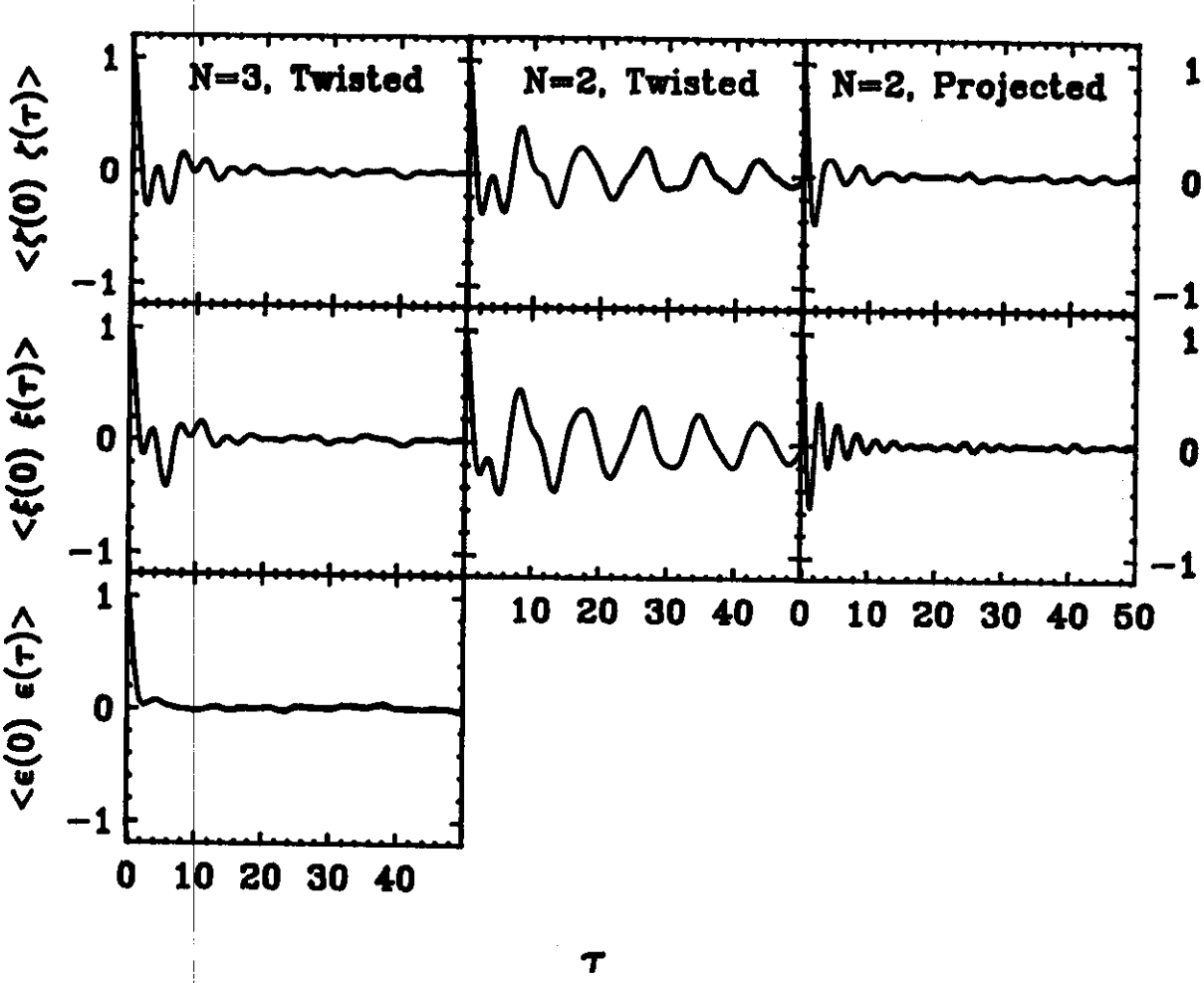

FIGURE 11. Same as Fig. 10, except auto-correlation functions are for the pseudofrictions.

interaction described by the Heisenberg Hamiltonian:

$$H = \kappa \sum_{i=1}^{50} \mathbf{J^i} \cdot \mathbf{J^{i+1}}. \tag{5.26}$$

The underlying algebra is the direct product of $N = 50$ $SU(2)$ algebras:

$$\mathcal{A} = \overbrace{SU(2) \otimes SU(2) \otimes ... \otimes SU(2)}^{\text{50 times}}. \tag{5.27}$$

The Lie-Poisson brackets in this direct product space are the obvious generalization

$$\{F(X), G(X)\} = \sum_{\mu=1}^{50} \epsilon_{ijk} J_k^\mu \frac{\partial F}{\partial J_i^\mu} \frac{\partial G}{\partial J_j^\mu}. \tag{5.28}$$

This system is coupled to the heat bath using the twisted method, resulting in the equations of motion:

$$\begin{aligned}
\dot{J}_i^\mu &= \epsilon_{ijk} J_k^\mu \left[\kappa (J_j^{\mu-1} + J_j^{\mu+1}) - h(\zeta) A_j(J^\mu) - g(\xi) B_j(J^\mu) \right], \\
\dot{\zeta} &= \alpha \sum_{\mu=1}^{50} \epsilon_{ijk} J_k^\mu \left[\kappa (J_j^{\mu-1} + J_j^{\mu+1}) A_j(J^\mu) - T \frac{\partial A_j(J^\mu)}{\partial J_i^\mu} \right], \\
\dot{\xi} &= \beta \sum_{\mu=1}^{50} \epsilon_{ijk} J_k^\mu \left[\kappa (J_j^{\mu-1} + J_j^{\mu+1}) B_j(J^\mu) - T \frac{\partial B_j(J^\mu)}{\partial J_i^\mu} \right],
\end{aligned} \tag{5.29}$$

where $i = 1, 2, 3$ and $\alpha = 1, ..., 50$. These $3 \times 50 + 2 = 152$ equations of motion have been evolved in time, using the generalization of Eq. (5.8):

$$A_k^\mu = (J_3^\mu, J_1^\mu, J_2^\mu), \qquad B_k^\mu = (J_2^\mu, -J_1^\mu, 0), \tag{5.30}$$

together with random initial spin configurations, a spin magnitude of unity, and $\alpha = \beta = T = 1$, using two pseudofrictions. The degree of thermalization is judged by the quality of the $f(\zeta)$ and $f(\xi)$ thermal distributions, for which the exact results are always known, shown in Fig. 12. Since this Hamiltonian is some sense linear in the generators, it is highly regular, and in principle an additional friction should be used to obtain a more rapid thermalization, such as the generalization of the function C in Eq. (5.8). A typical measurement, such as the spin-spin correlation function:

$$\left\langle (-)^k \mathbf{S_r} \cdot \mathbf{S_{r+k}} \right\rangle \tag{5.31}$$

is shown in Fig. 13.

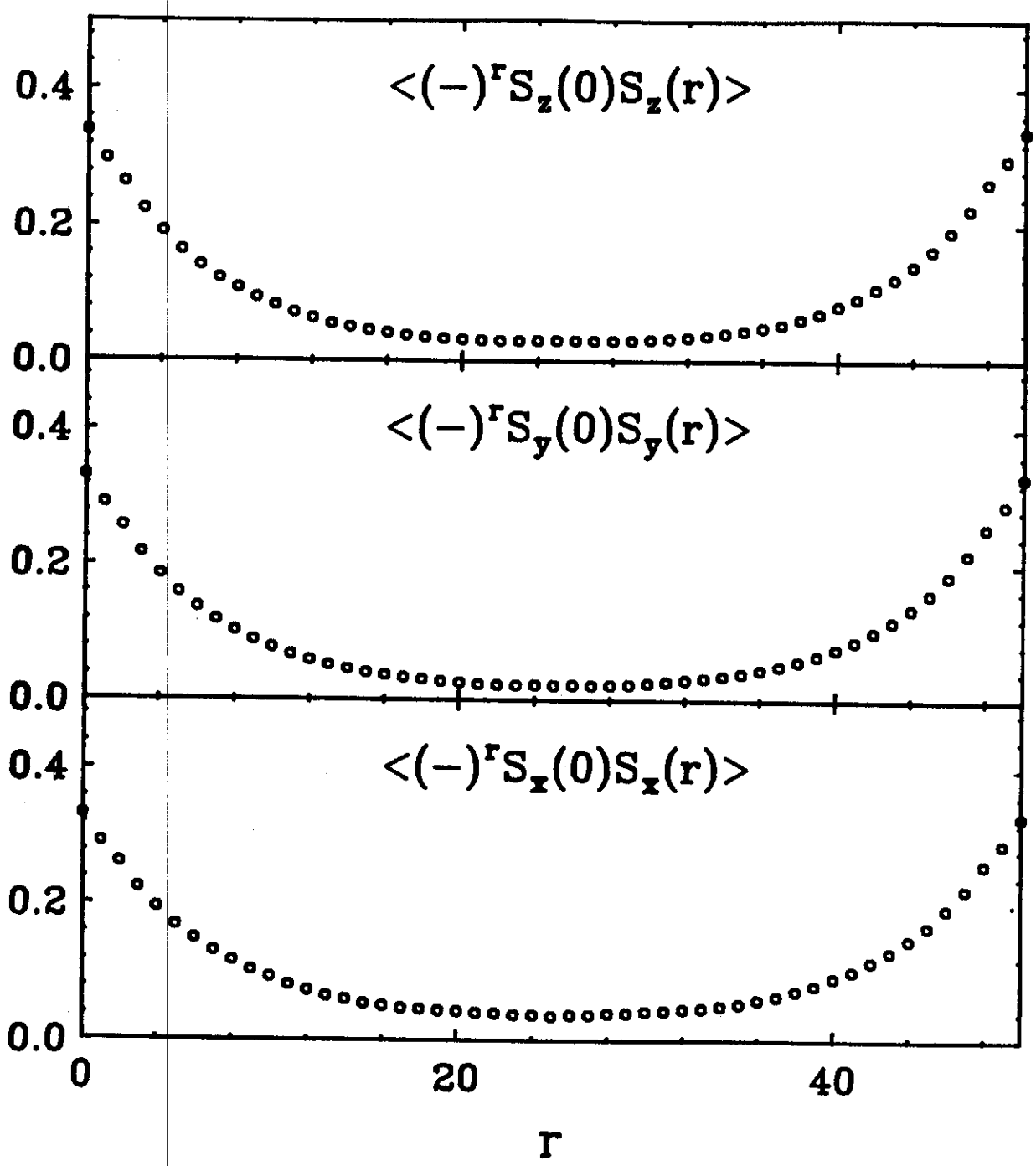

FIGURE 12. Convergence of the thermal distributions of the pseudofrictions to the exact result for 50 classical spins on a periodic chain. This can always be used as a guide for thermalization for general systems under study.

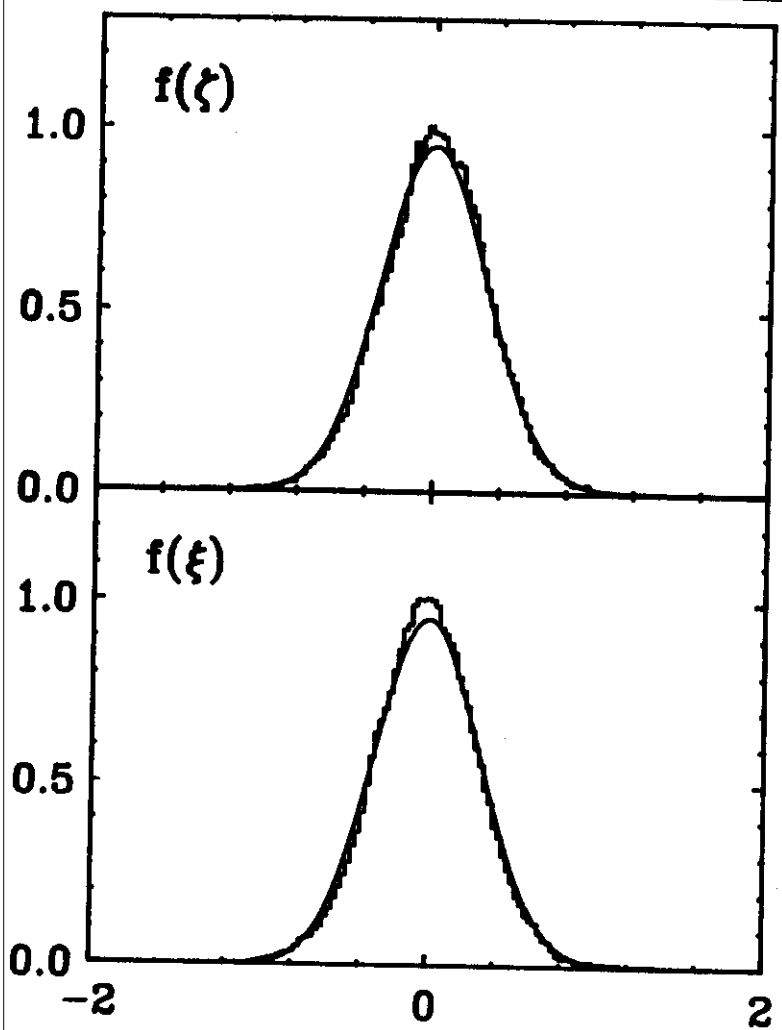

FIGURE 13. Spin-spin correlation functions for the classical Heisenberg antiferromagnet consisting of 50 spins on a periodic chain.

TABLE 3. Structure constants of $SU(3)$.

(i,j,k)	f_{ijk}	(i,j,k)	d_{ijk}
123	1	118,228,338	$\frac{1}{\sqrt{3}}$
147,246,257,345	$\frac{1}{2}$	146,157,256,344,355	$\frac{1}{2}$
156,367	$-\frac{1}{2}$	247,366,377	$-\frac{1}{2}$
458,678	$\frac{\sqrt{3}}{2}$	448,558,668,778	$-\frac{1}{2\sqrt{3}}$
		888	$-\frac{1}{\sqrt{3}}$

6. Hamiltonians with $SU(3)$ Symmetry

The Lie algebra $SU(3)$ is very useful since it contains the basic features of a general algebra, while still being simple enough to allow exact numerical computations. This symmetry is particularily fruitful in nuclear physics, as it describes the algebra of quadrupole excitations, the rudimentary ingredient in the study of collective nuclear structure.

6.1. Classical Limit

In order to discuss the classical limit of $SU(3)$, we first write the quantum commutators

$$\left[\hat{X}_i, \hat{X}_j\right] = i f_{ijk} \hat{X}_k, \qquad (i,j,k = 1,...,8) \tag{6.1}$$

where f_{ijk} is fully anti-symmetric, and its values are given in Table 3. There are 8 generators, $\hat{X}_i$, and two Casimir operators, $\hat{C}_2$ and $\hat{C}_3$, which are quadratic and cubic in the generators, respectively. The commutators of $\hat{C}_2$ and $\hat{C}_3$ vanish:

$$\left[\hat{X}_i, \hat{C}_{2,3}\right] \equiv 0. \tag{6.2}$$

The classical limit [10] is then defined through Eq. (2.2), and the equations of motion are given by the Lie-Poisson brackets $(i,j,k = 1,...,8)$

$$\dot{X}_i = \{X_i, H\} = \frac{\partial H}{\partial X_j} X_k c_{ijk} = G_{ij}(X) \frac{\partial H}{\partial X_j}. \tag{6.3}$$

The classical space for $SU(3)$ is an 8-dimensional Euclidian space spanned by the coordinates $(X_1,...,X_8)$, together with quadratic and cubic constraints (Casimir

functions) $C_2(X)$ and $C_3(X)$. These functions have zero Lie-Poisson bracket with arbitrary functions (Hamiltonians) of X, in analogy with Eq. (6.2)

$$\{X_i, C_{2,3}(X)\} \equiv 0. \tag{6.4}$$

Expliticly, $C_2(X)$ and $C_3(X)$ are written in terms of two fully symmetric tensors:

$$\begin{aligned} C_2 &= \frac{1}{2}\delta_{ij}X_iX_j = \frac{1}{2}\sum_{i=1}^{8} X_i^2, \\ C_3 &= \frac{1}{2}d_{ijk}X_iX_jX_k \\ &= -\frac{1}{24}[2\sqrt{3}X_8^3 + 3\sqrt{3}X_8(X_4^2 + X_5^2 + X_6^2 + X_7^2) \\ &\quad - 6\sqrt{3}X_8(X_1^2 + X_2^2 + X_3^2) - 9X_3(X_4^2 + X_5^2 - X_6^2 - X_7^2) \\ &\quad - 18(X_1X_5X_7 - X_2X_4X_7 + X_1X_4X_6 + X_2X_5X_6)]. \end{aligned} \tag{6.5}$$

The values of d_{ijk} are given in Table 3.

Our $SU(3)$ system can now be coupled to a heat bath using the methods of chapter 4. However, the form of the Casimir functions makes the projected method more prohibitive than the twisted method, since the gradients of these functions would appear in the (projected) equations of motion. For larger algebras, this can become quite cumbersome. Hence we use the twisted method. The equations of motion for a system described by an $SU(3)$ Hamiltonian $H(X)$, and coupled to a heat bath with two pseudofrictions, can be written using the twisted method as:

$$\begin{aligned} \dot{X}_i &= G_{ij}(X)\left(\frac{\partial H}{\partial X_j} - g_1(\zeta)A_j - g_2(\xi)B_j\right), \\ \dot{\zeta} &= \alpha G_{ij}(X)\left(A_j\frac{\partial H}{\partial X_i} - T\frac{\partial A_j}{\partial X_i}\right). \\ \dot{\xi} &= \beta G_{ij}(X)\left(B_j\frac{\partial H}{\partial X_i} - T\frac{\partial B_j}{\partial X_i}\right). \end{aligned} \tag{6.6}$$

6.2. Equations of Motion

The three-level Lipkin-Meshkov-Glick Hamiltonian is used to describe M particles in three $M-$fold degenerate quantum levels. It has the general form

$$\hat{H}_{LMG} = \sum_{k=1}^{3} E_k \left(\sum_{m=1}^{M} a_{km}^{\dagger} a_{km} \right) - \frac{1}{2} \sum_{k,l=1}^{3} V_{kl} \left(\sum_{m=1}^{M} a_{km}^{\dagger} a_{lm} \right)^2 , \tag{6.7}$$

where a_{kl} ($a_{kl}^{\dagger}$) annihilates (creates) particle l in level k. For simplicity, we consider $V_{kl} = V'$ for $k = l$, $V_{kl} = W'$, $k \neq l$. In terms of the generators of $SU(3)$, the LMG Hamiltonian can be rewritten as follows:

$$\begin{aligned} \hat{H}_{LMG} = \frac{1}{12} \Big(& 2\sqrt{3}\hat{X}_8(E_1 + E_2 - 2E_3) - 3V(\hat{X}_7^2 - \hat{X}_6^2 + \hat{X}_5^2 - \hat{X}_4^2 + \hat{X}_2^2 - \hat{X}_1^2) \\ & + W(3\hat{X}_8^2 + 3\hat{X}_3^2 + 2\hat{C}_1^2) + 6\hat{X}_3(E_1 - E_2) - 4\hat{C}_1(E_1 + E_2 + E_3) \Big), \end{aligned} \tag{6.8}$$

where E_1, E_2, E_3, W, V are constants and $\hat{C}_1$ is the number operator. (The explicit relation between W, V in Eq. (6.8) and V', W' in Eq. (6.7) is not important for our considerations.) Since the number operator $\hat{C}_1$ is an element of $U(3)$ and not $SU(3)$, we put $C_1 = 0$ in Eq. (6.8) (this can be achieved by a simple translation in X). The classical limit is realized by simply replacing the quantum operators by coordinates: $\hat{X}_k \to X_k$. If we choose

$$E_1 = E_2 = E_3, \qquad W = V, \tag{6.9}$$

the Hamiltonian has the form

$$H = \frac{V}{12} \left[8Q^2 + \frac{3}{2} L^2 \right], \tag{6.10}$$

where Q and L are the quadrupole and angular momentum generators of $SU(3)$. These generators are given in Appendix B. Eq. (6.10) is a crude model for nuclear collective excitations in deformed nuclei. Using the results of Appendix B, we can write Eq. (6.10) in a computationally simpler form:

$$H = \frac{V}{2} \left[C_2 - X_2^2 - X_5^2 - X_7^2 \right]. \tag{6.11}$$

Since C_2 is a constraint, only X_2, X_5 and X_7 play a dynamical role in the Hamiltonian. We will take Eq. (6.11) together with $V = 1$ as our Hamiltonian.

The equations of motion of this system coupled to the thermostat are then realized by choosing the vector functions A_i and B_i. A particular choice we have used is given by

$$\begin{aligned} A &= (2X_2, -2X_1, 0, X_5, -X_4, X_7, -X_6, 0), \\ B &= (X_6, X_7, X_8, X_1, X_2, X_3, X_4, X_5). \end{aligned} \tag{6.12}$$

We will also compare the results with two pseudofrictions to those using three pseudo frictions. For this case we have taken a third vector defined by

$$C = (X_5, X_3, X_1, X_8, X_2, X_4, X_6, X_7). \tag{6.13}$$

The three choices A, B and C satisfy the condition (4.4) that phase space volume is not conserved exactly:

$$G_{ij}\frac{\partial O_i}{\partial X_j} \neq 0, \tag{6.14}$$

where $O = A, B$ or C. Corresonding to these functions, we take the frictions

$$g_1(\zeta) = \zeta^3, \qquad g_2(\xi) = \xi, \tag{6.15}$$

and when we use three pseudofrictions,

$$g_3(\epsilon) = \epsilon. \tag{6.16}$$

This specifies completely the equations of motion and the thermal distributions.

It should be noted that the initial conditions specify the value of the Casimir constraints. This corresponds to defining the representation of $SU(3)$ to be investigated. Since, when integrating numerically the equations of motion the values of the constraints begin to wander, it is necessary to periodically check and renormalize the position $(X_1, ..., X_8)$ so as to preserve the constraints. For the spin systems that we have discussed up to now, the renormalization of the spin vector is trivial to perform. For higher dimensional spaces with more constraints, this requires additional effort, which can be handled case by case.

6.3. Thermal Distributions

We have studied the Hamiltonian (6.11), using the equations of motion (6.6), the functions A and B in (6.12) and the pseudofriction terms (6.15). All of our $SU(3)$ simulations in this section have been done with the initial conditions

$$(X_1,...,X_8,\zeta,\xi) = (-0.333,-0.45,0.984,0.559,0.189,-0.265,-0.595,-0.823,0,0), \tag{6.17}$$

which has the corresponding constraints

$$C_2 = 1.366, \qquad C_3 = -0.297. \tag{6.18}$$

The trajectory was evoled in time to the final time $t = 90000$, using the parameters $\alpha = \beta = T = 1$, and an integration time step of $dt = 0.1$. In Fig. 14 we present results obtained by binning the values of the coordinates X at each time step. It is equally simple to determine $f(Q)$ and $f(L)$ instead of $f(X)$, however we are not interested in the details of this model at the moment.

The exact distribution functions can be found using the method outlined in Appendix C. The solid lines in Fig. 14 correspond to numerical integration of the thermal expectation values of X_i for $i = 1,3,4,6,8$

$$f(X_k) = \int \prod_{i=1}^{8} dX_i\, d\zeta d\xi\, \delta(C_2(X) - C_2)\, \delta(C_3(X) - C_3)\, e^{-H/T}\, X_k. \tag{6.19}$$

For X_2, X_5 and X_7 the exact distributions are more difficult to evalutate, and we have not done so.

The exact distribution for the pseudofrictions ζ and ξ are always known, and these are compared to the results of the simlation in Fig. 15. The convergence is clearly quite good. Further, if we histogram the value of the Hamiltonian, we can compute the energy distribution $f(E,T)$, at this temperature. This is shown in Fig. 16. From distributions of this type, it is possible to determine the density of states for this model by unfolding $f(E,T)$ with the Boltzmann factor

$$\rho(E) = e^{E/T} f(E,T). \tag{6.20}$$

By piecing several overlapping distributions, $f(E,T_1), f(E,T_2),...$, determined at selected temperatures T_i, the density of states $\rho(E)$ can be determined over a wide range of energies for this simple nuclear model. In Figs. 17-18, we show the results of the simluation for $T = 0.1$. The thermal distributions can be seen to undergo a strong change in character, and the energy distribution $f(E, T = 0.1)$ is becoming peaked near the ground state energy.

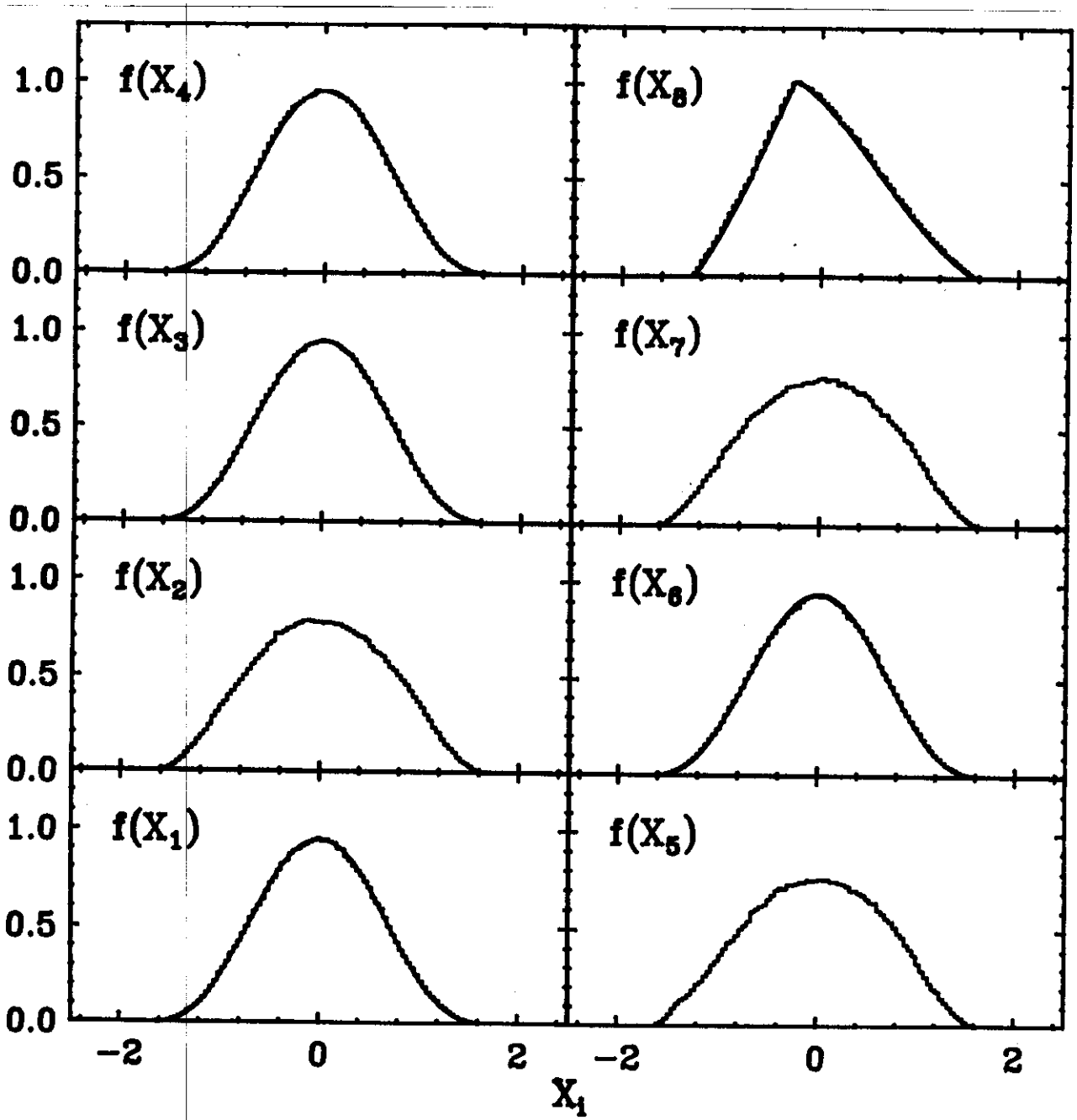

FIGURE 14. Comparison between exact and computed thermal distributions for the simple nuclear collective $SU(3)$ Hamiltonian $H = Q^2/3 + L^2/8$. The parameters are $\alpha = \beta = T = 1$.

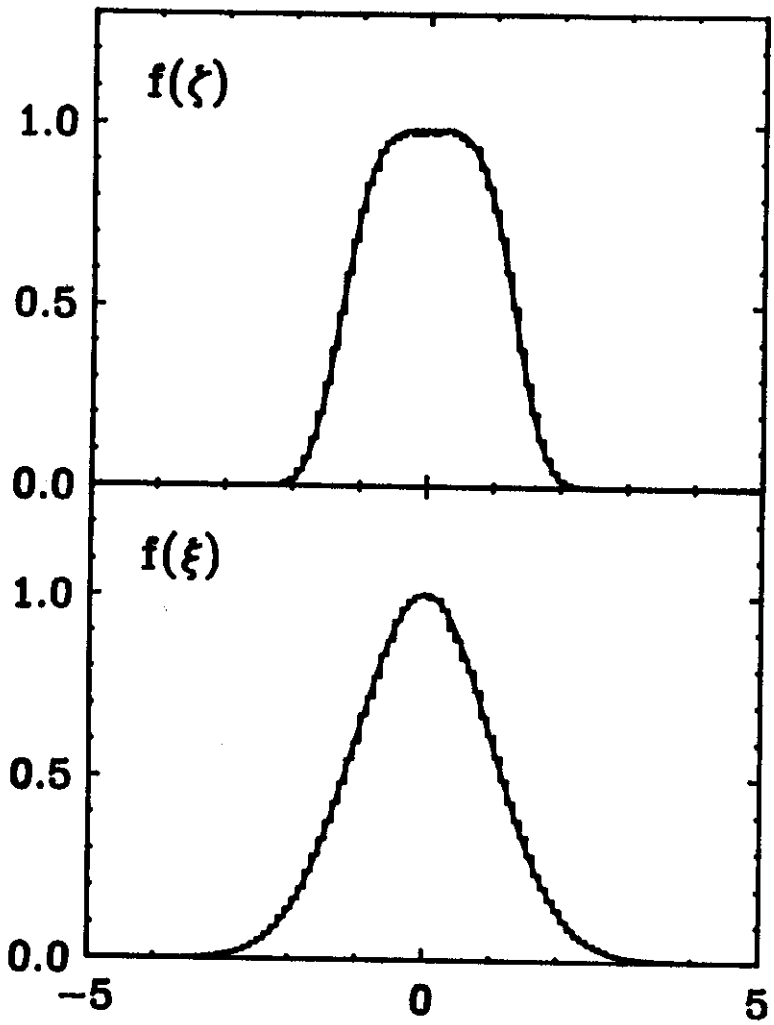

FIGURE 15. Comparison between exact and computed thermal distributions for ζ and ξ corresponding to Fig. 14.

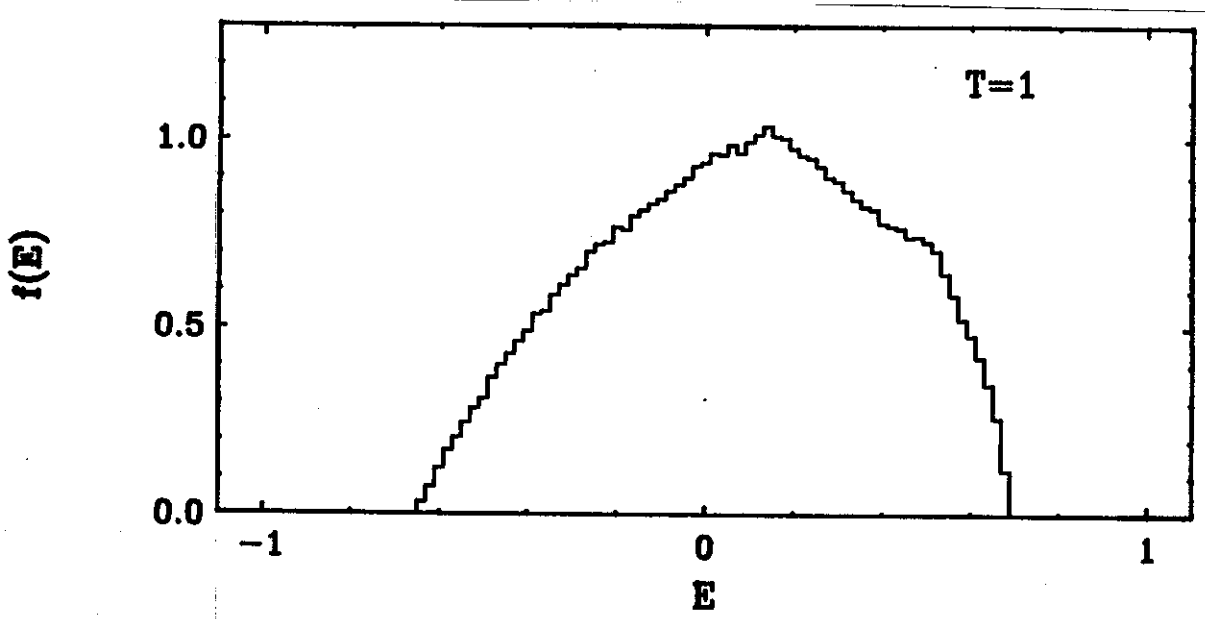

FIGURE 16. Energy distribution of the nuclear Hamiltonian, corresponding to Fig. 14.

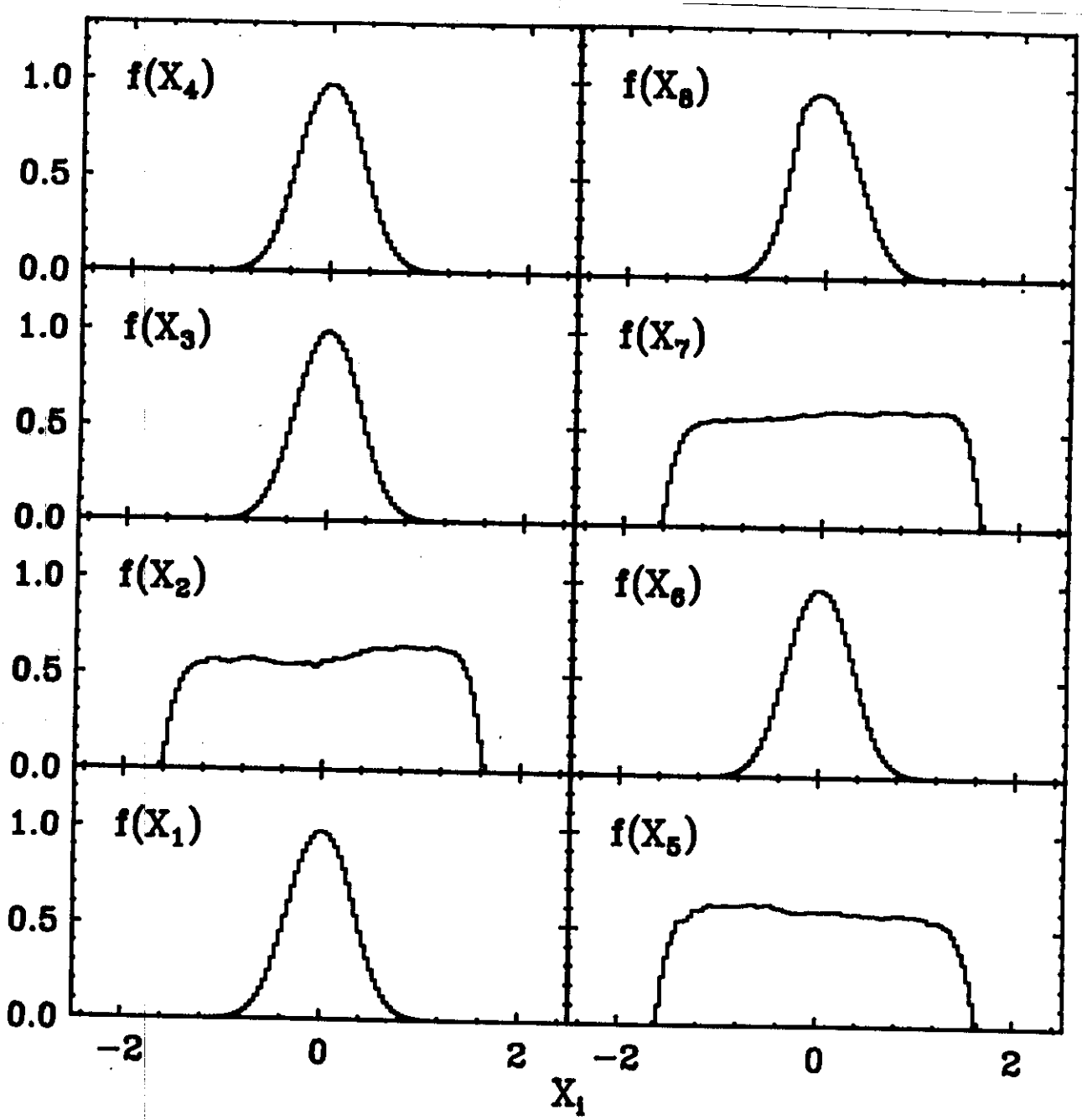

FIGURE 17. Same as Fig. 14 except $T = 0.1$.

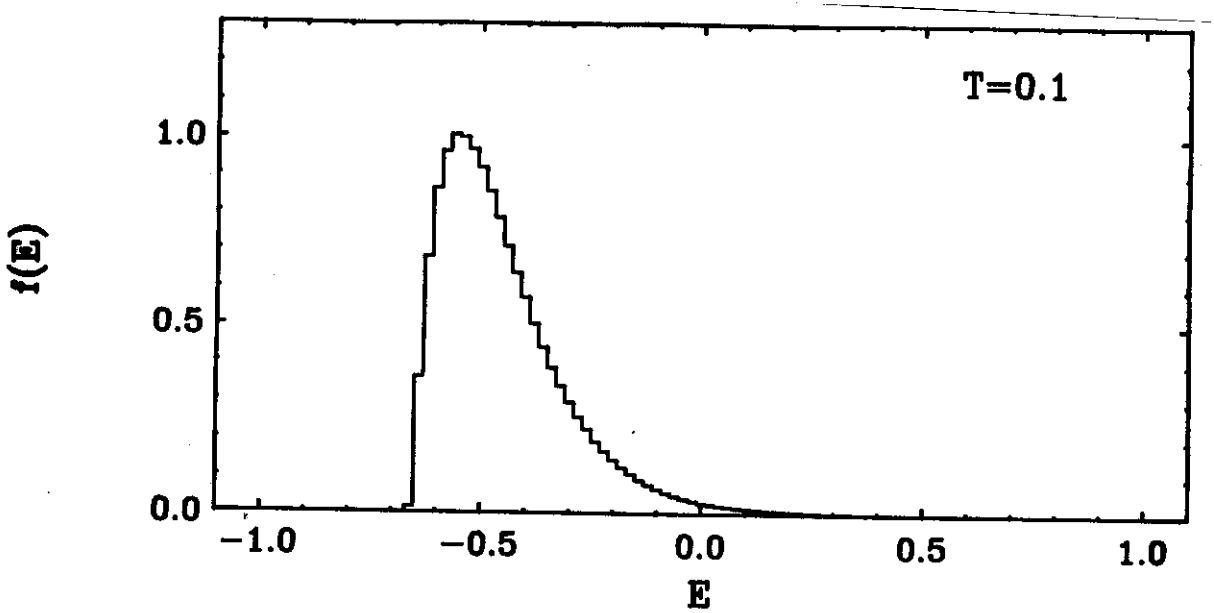

FIGURE 18. Same as Fig. 16 except $T = 0.1$.

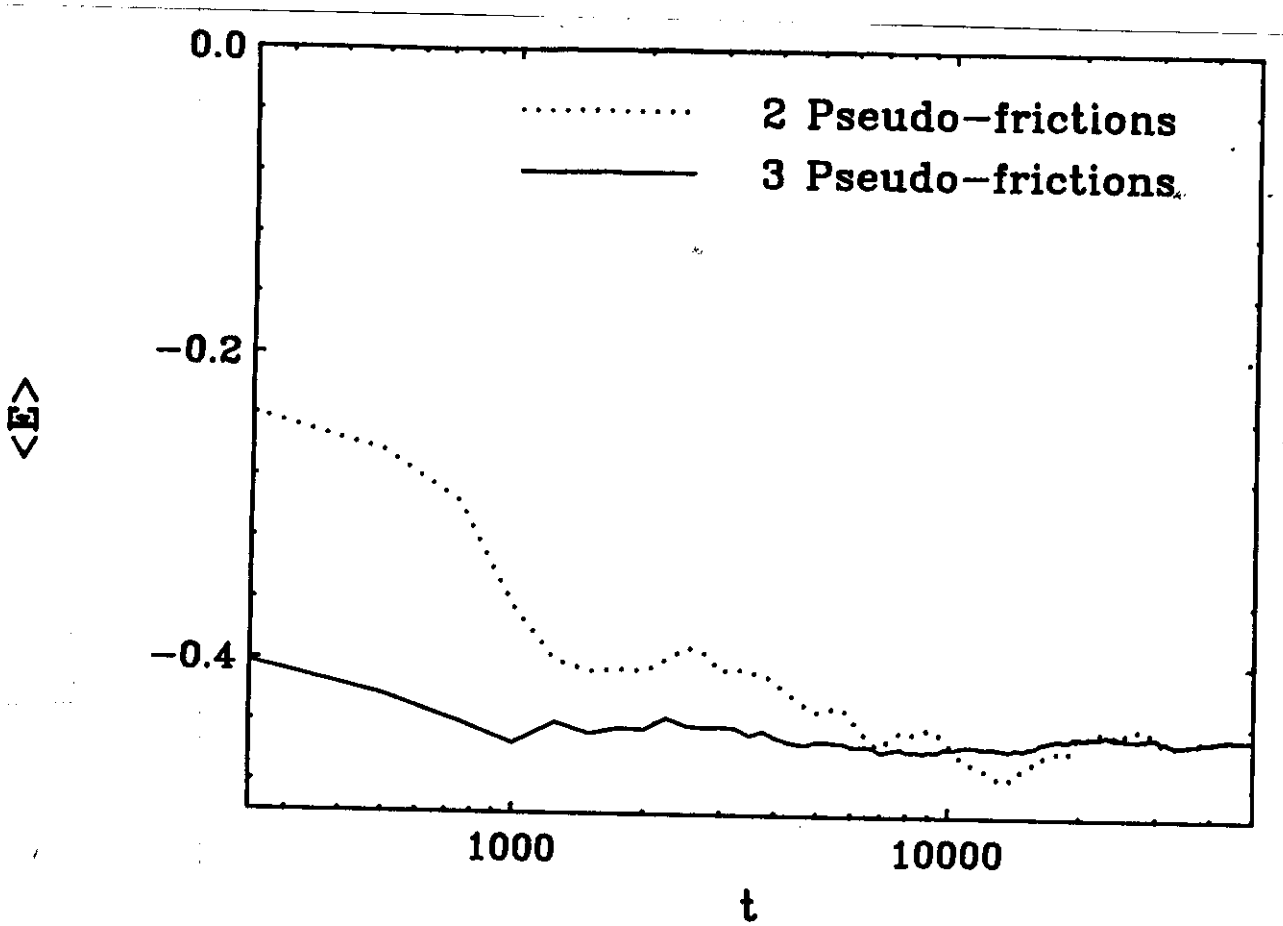

FIGURE 19. Convergence comparison between two (dots) and three (solid) pseudofrictions for the $SU(3)$ Hamiltonian $H = Q^2/3 + L^2/8$. Clearly the additional frictions improves thermalization.

6.4. Two and Three Pseudofrictions

In principle, we are free to add as many pseudofriction functions as we want to the equations of motion. In Fig. 19 we compare the results of simulations using two and three pseudofriction functions. The dotted line corresponds to the two pseudofriction ($N = 2$) case discussed above with $T = 0.1$. The solid line corresponds to the addition of the third pseudofriction C listed in Eqs. (6.13), (6.16), with the same initial conditions together with $\epsilon = 0$. As one can see, the additional pseudofriction significantly improves the rate of thermalization. The equilibrium value of $< E >$ corresponds to the mean of the distribution $f(E, T = 0.1)$ in Fig. 18.

In principle one can extend this discussion to a classical lattice in which each site has an $SU(3)$ internal symmetry group associated with it, in the same way that we studied the classical spin chains. This provides a new technique to study classical $SU(3)$ lattice models at finite temperatures.

7. Conclusions

We have presented a method in which the canonical ensemble properties can be computed for constrained dynamical systems. Since this method reduces to our previous methods in I for the case of a trivial Poisson tensor, it is an approach which is applicable to general dynamical systems. Examples of the method have been drawn from systems with internal Lie algebra symmetries for the sake of presentation. Extensions of these methods to other physical systems with constrained dynamics is straightforward. One clear advantage of the methods presented in this paper is their obvious generalization to non-equlibrium situations. From our previous experience we expect that this type of approach will compare quite favorably with the best existing scheme for computing equlibrium properties. In the case of the XY-model [9] we showed that the present approach leads to a better handling of the so called critical slowing down than the hybrid Monte Carlo method. On the other hand, on can safely say that the isothermal (chaotic) dynamics is still in its infancy and its potential has yet to be explored.

Support was provided by the National Science Foundation under Grant Nos. 87-14432 and 89-06670.

APPENDIX A

In this appendix we provide the details of the computation of the equations of motion for the pseudofriction functions from the Liouville continuity equation, using the twisted method. For a general Lie algebra in the classical limit, we defined the equations of motion of the system plus heat bath in Eq. (4.3b) as

$$\dot{X}_i = c_{ijk} X_k \left\{ \frac{\partial H}{\partial X_j} - g(\zeta) A_j \right\}. \tag{A.1}$$

In the Liouville equation (4.8), we must compute the phase space derivative of $\dot{X}_i$. We will now see that, when using the twisted method,

$$\frac{D\dot{X}_i}{DX_i} = \frac{\partial \dot{X}_i}{\partial X_i}. \tag{A.2}$$

By direct substitution, using Eq. (2.7), we have

$$\frac{D\dot{X}_i}{DX_i} = \frac{\partial \dot{X}_i}{\partial X_i} - \sum_{\alpha=1}^{n} e_i^\alpha e_k^\alpha \frac{\partial \dot{X}_i}{\partial X_k}. \tag{A.3}$$

Lets expand explicitly the term involving the sum in (A.3). Inserting (A.1) in that term yeilds

$$\sum_{\alpha=1}^{n} e_i^\alpha e_k^\alpha c_{ilm} X_m \left\{ \frac{\partial^2 H}{\partial X_k X_l} - g(\zeta) \frac{\partial A_l}{\partial X_k} \right\}. \tag{A.4}$$

This term vanishes, independent of the term in the brackets. This is simply due to the fact that the matrix $c_{ijk}X_k$ has a zero eigenvalue when contracted with a gradient of a Casimir function. From Eq. (2.12) we found that

$$0 = c_{ijk} \frac{\partial C^\alpha}{\partial X_i} X_k \, \mathcal{G}_j(X), \tag{A.5}$$

where $\mathcal{G}_j(X)$ is an aribtrary function. So equivalently we have

$$0 = c_{ijk} e_i^\alpha X_k \, \mathcal{G}_j(X). \tag{A.6}$$

Thus we establish (A.2). The Liouville equation is now

$$\begin{aligned} 0 &= \frac{\partial (f\dot{X}_i)}{\partial X_i} + \dot{\zeta} \frac{\partial f}{\partial \zeta} \\ &= c_{ijk} X_i \left(-g(\zeta) \frac{\partial A_j}{\partial X_i} - \frac{1}{T} \frac{\partial H}{\partial X_i} g(\zeta) A_j \right) - \frac{1}{\alpha T} \dot{\zeta} \frac{\partial G(\zeta)}{\partial \zeta}. \end{aligned} \tag{A.7}$$

Here we have used the ansatz $d\dot{\zeta}/d\zeta = 0$ and the distribution f given in Eq. (4.5). Solving this for $\dot{\zeta}$ then gives the results of Eq. (4.13).

APPENDIX B

The relation of the generators of $SU(3)$, which satisfy $\{X_i, X_j\} = f_{ijk} X_k$, to the spherical tensor components of the quadrupole tensor Q_μ and the angular momentum operator L_μ introduced in chapter 6 is given by

$$\begin{aligned}
Q_0 &= -\sqrt{\frac{3}{2}} X_8, \\
Q_1 &= -\frac{\sqrt{3}}{2}(X_4 + iX_6), \\
Q_{-1} &= -\frac{\sqrt{3}}{2}(-X_4 + iX_6), \\
Q_2 &= \frac{\sqrt{3}}{2}(X_3 + iX_1), \\
Q_{-2} &= \frac{\sqrt{3}}{2}(X_3 - iX_1).
\end{aligned} \qquad \begin{aligned}
L_0 &= 2X_2, \\
L_1 &= -\sqrt{2}(X_7 - iX_5), \\
L_{-1} &= \sqrt{2}(X_7 + iX_5),
\end{aligned} \tag{B.1}$$

These generators satisfy the usual Elliott $SU(3)$ commutation relations, or equivalently, Lie-Poisson brackets:

$$\begin{aligned}
\{L_\mu, L_\nu\} &= -\sqrt{2}\,\langle 1\mu\, 1\nu \mid 1\rho\rangle\, L_\rho, \\
\{Q_\mu, Q_\nu\} &= \frac{3\sqrt{10}}{8}\,\langle 2\mu\, 2\nu \mid 1\rho\rangle\, L_\rho, \\
\{Q_\mu, L_\nu\} &= -\sqrt{6}\,\langle 2\mu\, 1\nu \mid 2\rho\rangle\, Q_\rho,
\end{aligned} \tag{B.2}$$

where the symbol in braces is a Clebsch-Gordan coefficient. The Casimir operators are

$$\begin{aligned}
C_2 &= \frac{2}{3}\left[\frac{3}{4}(L_0^2 - 2L_1L_{-1}) + 2(Q_0^2 - 2Q_1Q_{-1} + 2Q_2Q_{-2})\right], \\
C_3 &= -\frac{1}{36}\Big[2\sqrt{2}Q_0\,(9L_0^2 - 8Q_0^2 + 48Q_2Q_{-2}) + 6\sqrt{2}Q_0\,(3L_1L_{-1} + 8Q_1Q_{-1}) \\
&\quad - 18\sqrt{6}L_0\,(L_1Q_{-1} + L_{-1}Q_1) + 18\sqrt{3}\,(L_1^2Q_{-2} + L_{-1}^2Q_2) \\
&\quad - 48\sqrt{3}\,(Q_{-2}Q_1^2 + Q_2Q_{-1}^2)\Big].
\end{aligned} \tag{B.3}$$

APPENDIX C

Integration of the $SU(3)$ Hamiltonian can be performed numerically if we use the variables introduced recently by Johnson [12]

$$\begin{aligned}
X_3 &= p_1, \\
X_8 &= p_2, \\
\sqrt{X_1^2 + X_2^2 + X_3^2} &= p_3, \\
X_1 + iX_2 &= \exp(iq_1)\sqrt{p_3^2 - p_1^2}, \\
X_4 + iX_5 &= \exp[\frac{i}{2}(q_1 + \sqrt{3}q_2 + q_3)]\sqrt{p_3 + p_1}A \\
&\quad + \exp[\frac{i}{2}(q_1 + \sqrt{3}q_2 - q_3)]\sqrt{p_3 - p_1}B, \\
X_6 + iX_7 &= \exp[\frac{i}{2}(-q_1 + \sqrt{3}q_2 + q_3)]\sqrt{p_3 - p_1}A \\
&\quad - \exp[\frac{i}{2}(-q_1 + \sqrt{3}q_2 - q_3)]\sqrt{p_3 + p_1}B,
\end{aligned} \tag{C.1}$$

where

$$\begin{aligned}
A &= \frac{1}{2p_3}\{(\frac{P-Q}{3} + p_3 + \frac{p_2}{\sqrt{3}})(\frac{P+2Q}{3} + p_3 + \frac{p_2}{\sqrt{3}})(\frac{2P+Q}{3} - p_3 - \frac{p_2}{\sqrt{3}})\}^{1/2}, \\
B &= \frac{1}{2p_3}\{(\frac{Q-P}{3} + p_3 - \frac{p_2}{\sqrt{3}})(\frac{P+2Q}{3} - p_3 + \frac{p_2}{\sqrt{3}})(\frac{2P+Q}{3} + p_3 - \frac{p_2}{\sqrt{3}})\}^{1/2}.
\end{aligned} \tag{C.2}$$

Here P, Q are linked to the Casimir functions as follows:

$$\begin{aligned}
C_2 &= \frac{1}{6}[P^2 + Q^2 + PQ], \\
C_3 &= \frac{1}{72}(P-Q)(2P+Q)(P+2Q).
\end{aligned} \tag{C.3}$$

The $SU(3)$ measure (for the algebra, not group) can be written as

$$dX_1 \cdots dX_8 = \frac{(P+Q)PQ}{16\sqrt{3}} dq_1 dq_2 dq_3 dp_1 dp_2 dp_3 dP dQ \tag{C.4}$$

In the new coordinates, the constraints C_2 and C_3 are related only to P and Q. Integrals over the phase space then only depend on the six coordinates p_i and q_i.

Integration over the $SU(3)$ measure (for the algebra, not group) can done if we define

$$u = (\sqrt{3}q_2 + q_3)/2, \qquad v = (\sqrt{3}q_2 - q_3)/2, \tag{C.5}$$

where $0 \leq u, v, q_1 \leq 2\pi$. For the p_i, define

$$w = \frac{p_2}{\sqrt{3}} + p_3, \qquad x = \frac{p_2}{\sqrt{3}} - p_3. \tag{C.6}$$

The limits of integration of w, x are determined by the roots of A, B in (C.2). These are in turn related to the Casimir functions (C.3) through the initial conditions. p_1 has the limits $-p_3 \leq p_1 \leq p_3$.

REFERENCES

1. A.Bulgac and D.Kusnezov, Phys. Rev. **A42**, 5045 (1990) .
2. D.Kusnezov, A.Bulgac and W.Bauer, Ann. Phys. **204**, 155 (1990).
3. D.Kusnezov and A.Bulgac, (submitted).
4. S. Nosé, J. Chem. Phys. **81**, 511 (1984); Mol. Phys. **52**, 255 (1984), W. G. Hoover, Phys. Rev. **A 31**, 1695 (1985); *Molecular Dynamics*, Lecture Notes in Physics (Springer-Verlag, New York, 1986), Vol. 258; H. A. Posch, W. G. Hoover and F. J. Veseley, Phys. Rev. **A 33**, 4253 (1986).
5. A.Bulgac and D.Kusnezov, Phys. Lett. **A151**, 122 (1990).
6. N.Metropolis, A.W.Rosenbluth, M.N.Rosenbluth, A.H.Teller and E.Teller, J. Chem. Phys. **21**, 1087 (1953).
7. G.Parisi and Wu Yongshi, Scientia Sinica, **24**, 283 (1981).
8. S.Duanne, A.D.Kennedy, B.J.Pendleton and D.Roweth, Phys. Lett. **B195**, 216 (1987).
9. J.H.Sloan, D.Kusnezov and A.Bulgac, to be submitted.
10. A.Bulgac and D.Kusnezov, Ann. Phys. **199**, 187 (1990).
11. P.A.M.Dirac, *Lectures in Quantum Mechanics*, Vol. 2.
12. K.Johnson, Ann. Phys. **192** 104 (1989).
13. A.Trayanov and B.Müller, Duke University preprint (1991).
14. P.J.Olver, *Applications of Lie Groups to Differential Equations*, (Springer-Verlag, New York, 1986).
15. E.T.Whittacker, *Analytical Dynamics of Particles and Rigid Bodies*, Cambridge University Press, 1970, p. 322.
16. See for example V.Arnol'd and A.Avez, *Ergodic Problems of Classical Mechanics*, Addison-Wesley 1968.
17. T.E.Hull, W.H.Enright and K.R.Jackson, *User's guide for DVERK - A subroutine for solving non-stiff ODEs*, Department of Computer Science Technical Report 100, University of Toronto (1976); K.R.Jackson, W.H.Enright and T.E.Hull, *A theoretical criterion for comparing Runge-Kutta formulas*, Department of Computer Science Technical Report 101, University of Toronto (1977).
18. See for example, H.G.Schuster, *Deterministic Chaos: An Introduction*, (VCH, FRG, 1988), pp.114-115.